Extreme mobility creates contrasting patterns of panmixia, isolation-by-distance and hybridization in four flying-fox species (*Pteropus*)

Armin Scheben[1*], Adam McKeown[2], Tom Walsh[3], David A. Westcott[4], Suzanne S. Metcalfe[5], Eric P. Vanderduys[5] and Bruce L. Webber[6*]

[1] Simons Center for Quantitative Biology, Cold Spring Harbor Laboratory, Cold Spring Harbor, NY, 11724, United States of America
[2]CSIRO Environment, Adelaide, South Australia, 5052, Australia
[3]CSIRO Environment, Canberra, Australian Capital Territory, 2600, Australia
[4]CSIRO Environment, Atherton, Queensland, 4883, Australia; Present address: PO Box 1056, Atherton, Queensland, 4883, Australia
[5]CSIRO Environment, Brisbane, Queensland, 4102, Australia
[6]CSIRO Health and Biosecurity, Floreat, Western Australia 6014, Australia; School of Biological Sciences, University of Western Australia, Crawley, Western Australia 6009, Australia

*To whom correspondence should be addressed: armin.scheben@gmail.com, bruce.webber@csiro.au

Abstract

Speciation results from shifts between genetic connectivity and isolation of populations. Flying-foxes (*Pteropus*) are a compelling model to study the interplay of these evolutionary processes due to their rapid radiation in the island-rich region of the Indo-Australian Archipelago. Here, we investigate the population genetics of the highly mobile flying-foxes *Pteropus alecto*, *P. conspicillatus*, *P. poliocephalus*, and *P. scapulatus* across large parts of their overlapping ranges in Australia, Indonesia, and New Guinea. Using reduced-representation sequencing, we examined the extent to which panmixia, isolation-by-distance, and hybridization shaped these populations. Phylogenetic and demographic modeling approaches indicate that isolation-by-distance, despite ongoing gene flow, is prevalent in *P. alecto* and *P. conspicillatus* populations while *P. poliocephalus* and *P. scapulatus* are panmictic across Australia. We further find that hybridization and asymmetric gene flow from *P. conspicillatus* to *P. alecto* plays a role in

shaping the historic and contemporary populations of these recently diverged species, which exhibit gene flow along a geographic ring connecting Indonesia to Australia and New Guinea. We also uncover cryptic speciation within *P. alecto*, highlighting its complex evolutionary history. Together, our findings indicate that long-range population connectivity and limited restrictions on gene flow have shaped the evolution and diversification of flying-foxes.

1 Introduction

Dispersal shapes the evolutionary trajectory of species, both promoting speciation through geographic isolation and counteracting it by maintaining genetic connectivity (Lomolino, 2000). For instance, many species capable of long-distance dispersal form panmictic populations across continents (Bruxaux et al., 2024; Neethling et al., 2008; Peel et al., 2013; Reich et al., 2024; Reudink et al., 2011). In contrast, genetic isolation-by-distance is also widespread, leading to correlations between populations' geographic structure and their genetic structure (Aguillon et al., 2017; Sharbel et al., 2000; Wright, 1943). Panmixia and isolation-by-distance can occur within species at various spatiotemporal scales and incipient speciation can be prevented by secondary contact if populations are not sufficiently reproductively isolated. Alternatively, secondary contact can lead to reinforcement of species boundaries, and long-lasting natural hybrid zones can even be maintained despite gene flow across large geographic distances (Abbott et al., 2013). In rare cases, reproductively isolated populations connected by interbreeding populations around geographic barriers may form "ring species" (Irwin et al., 2005). However, our understanding of these complex stages of dispersal and speciation remains limited by how rarely these processes have been investigated in recently diverged highly mobile species.

Bats are the only mammals capable of powered flight and make up the second-most species-rich mammal group with 1,487 species (Simmons & Cirranello, 2025). Flying-foxes (*Pteropus*; Pteropodidae) are a particularly fast-radiating and recently diverged genus of bats originating in the Wallacea region of the Indo-Australian Archipelago (Tsang et al., 2020). The rapid diversification of flying-foxes has been associated with their high dispersal rate even compared to other volant species (Tsang et al., 2020) and their origin among archipelagos favoring allopatric speciation (Smyčka et al., 2023). Individual flying-foxes are capable of long-distance

movements (Breed et al., 2010; Eby, 1991; Westcott et al., 2015), with tracking experiments showing some individuals covering over 100 km a day (Roberts et al., 2012) and an average of 1,427-6,073 km annually (Welbergen et al., 2020). Flying-fox biogeography reflects this extreme mobility, with repeated colonisations of remote oceanic islands (O'Brien et al., 2009) and resulting insular, and often disjunct, distributions. While all Australian flying-fox species are known to make long-distance movements, the frequency of these movements is poorly described and their outcomes are as yet unknown. This means the extent and frequency of connectivity between different parts of species' ranges, how this is influenced by geography, and the evolutionary consequences are virtually unknown.

Four flying-fox species are native to the Australian mainland: the black flying-fox (*Pteropus alecto*), spectacled flying-fox (*P. conspicillatus*), grey-headed flying-fox (*P. poliocephalus*), and little-red flying-fox (*P. scapulatus*). While *P. poliocephalus* is endemic to Australia, the other species have disjunct distributions extending to Indonesia and New Guinea (Figure 1). An early genetic study using protein electrophoresis found that the widespread Australian *P. alecto*, *P. poliocephalus*, and *P. scapulatus* were panmictic, suggesting these bats resembled migratory species (Webb & Tidemann, 1996). The less widely distributed *P. conspicillatus* has a notably smaller population size compared to the other species and is listed as endangered in Australia (Roberts et al., 2020). Previous work has hypothesized that hybridization occurs between Australian *P. alecto* and both *P. conspicillatus* (Fox, 2006; Neaves et al., 2018) and *P. poliocephalus* (Webb & Tidemann, 1995) but not the more diverged *P. scapulatus*, based on small numbers of samples and limited genetic evidence. Although it has long been clear that *P. alecto* and *P. conspicillatus* are morphologically and genetically highly similar, their phylogenetic relationship has been resolved inconsistently across a number of studies using small sets of nuclear and mitochondrial genes (Almeida et al., 2009, 2014; Almeida, 2020; Fox, 2006; Tsang, 2015; Tsang et al., 2020). One phylogenetic study found that *P. alecto* sometimes nested within *P. conspicillatus*, explaining this through incomplete lineage sorting or hybridization (Almeida et al., 2009). Their divergence-time is variously estimated at 1-2 million years ago (mya) (Tsang, 2015) or 2-3 mya (Tsang et al., 2020). Intriguingly, their geographic distribution across Australia, Indonesia and New Guinea suggests that *P. alecto* and *P. conspicillatus* may represent a ring species that has not completely separated.

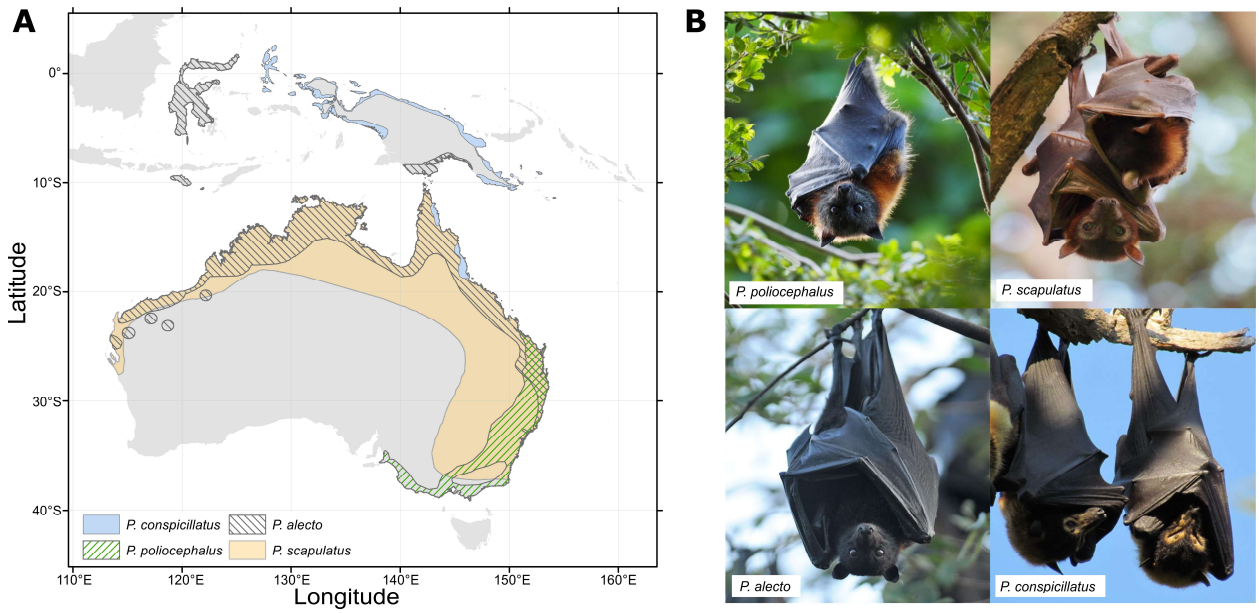

Figure 1. Sampled *Pteropus* flying-fox species and their geographic distributions. A) Ranges of the four flying-fox species native to the Australian mainland (https://www.iucnredlist.org). B) Photographs of the four flying-fox species. Image credit: Adam McKeown and Eric P. Vanderduys.

In this work, we investigate the population genetic structure of *P. conspicillatus*, *P. alecto*, *P. poliocephalus*, and *P. scapulatus* using genome-wide SNPs. We aim to determine 1) how panmixia and isolation-by-distance have shaped the genetic structure of these four flying-fox species across their distributions, 2) what role hybridization has played in their evolution, and 3) whether *P. alecto* and *P. conspicillatus* form a ring species. We hypothesize that mainland Australian flying-fox populations are panmictic, but that Indonesian populations of *P. alecto* and New Guinean populations of *P. conspicillatus* are genetically distinct from Australian populations. In addition, we hypothesize that *P. alecto* hybridizes with the related flying-fox species *P. conspicillatus* and *P. poliocephalus* in regions of overlapping distribution. Finally, we hypothesize that *P. alecto* and *P. conspicillatus* form an interbreeding population with gradual isolation-by-distance along the geographic ring connecting northern Australia with Indonesia, and New Guinea. Both species occur in Central Indonesia with *P. alecto* in Sulawesi and *P. conspicillatus* in the adjacent Moluccas. *P. alecto*'s distribution then extends south and meets *P. conspicillatus*, whose distribution spreads east into New Guinea, in eastern Australia and southern New Guinea. If this is a ring species, we would predict increasing divergence from Sulawesi and the Moluccas and diminishing divergence in the zone of overlap in northern

110 Australia and southern New Guinea. We expect that limits to dispersal over water barriers have
111 played a more important role in reducing gene flow than land barriers in northern Australia.

112 2 Materials and methods

113 2.1 Sample collection

114 Small 3mm circles of skin were removed from the wing membrane of individual flying-foxes
115 using a biopsy punch. The animals were captured in accordance with animal ethics approval
116 (Permit number CSIRO AEC 2016-17). Wing punches were obtained from individuals of the
117 four different flying-fox species, *P. alecto*, *P. poliocephalus*, *P. scapulatus*, and *P.*
118 *conspicillatus*. A total of 242 flying-fox samples were collected from 27 roost locations in
119 Australia and Papua New Guinea as well as 4 locations in Indonesia (Table S1). The samples
120 included 24 historical *P. alecto* specimens collected between 1989 and 2003 from the Western
121 Australian museum collection (WAM). Samples were stored in 80% ethanol at room temperature
122 until processing. Genomic DNA was extracted using the Qiagen DNA Blood and Tissue Kit
123 (Hilden, Germany) with an overnight incubation at 56°C until the tissue was completely lysed.

124 2.2 Double digest restriction site associated DNA sequencing (ddRAD) library
125 preparation

126 A total amount of 100 ng of genomic DNA from each individual was digested in a 50 µL
127 reaction with 20 units each of high-fidelity restriction enzymes, *PstI* and *EcoRI* (New England
128 Biolabs, Ipswich MA, USA), 10x Cut smart buffer and water for 30 min at 37°C, followed by a
129 heat inactivation step for 20 min at 65°C. The digestion products were allowed to slowly cool to
130 room temperature and held at 4°C. The digestion product was ligated to the modified P1 and P2
131 adapters ensuring that each individual had a unique combination of P1 and P2 barcodes. This
132 way twenty-four P1 and four P2 adapters allowed for multiplexing 96 individuals. The ligation
133 reactions were set up in 70 µL volume using the full volume of digestion product with 4 µL of
134 50 nM P1 and 12 µL of 50 nM P2 adapters, 2000 units of T4 DNA ligase (New England Biolabs,
135 Ipswich MA, USA), 0.15 mM rATP (Promega, Madison, WI, USA), and water and were
136 incubated for 30 min at 22°C. Ligations were heat inactivated for 20 mins at 65°C and allowed to

137 slowly cool to room temperature and held at 4°C. Ten µL of adapter-ligated DNA fragments
138 from all individuals were pooled, with careful mixing after each sample addition. The pooling
139 was replicated in three tubes and the following size-selected steps conducted to each tube
140 separately.

141 The larger fragments were extracted with 0.65x volume of Agencourt® AMPure® XP magnetic
142 bead solution (Beckman Coulter, Brea, CA, USA) and the bead discarded. The eluent was
143 transferred to a new tube, cleaned with 0.1x volume of bead solution, washed twice with 200 µL
144 of freshly made 80% ethanol, air-dried and resuspended in 20 µL elution buffer (Qiagen, Hilden,
145 Germany). The three replicates were then pooled and well mixed. Finally, 15 µL of size selected
146 DNA was used as a template in a 60µL PCR reaction with 30 µL of Phusion High Fidelity 2x
147 Master Mix (New England Biolabs, Ipswich MA, USA, 3 µL of 10 µM P1
148 (AATGATACGGCGACCACCGAGATCTACACTCTTTCCCTACACGACG) and P2
149 (CAAGCAGAAGACGGCATACGAGATCGTGATGTGACTGGAGTTCAGACGTGTGC)
150 primers and water. PCR conditions were: 98°C for 30 s, 20 cycles of 98°C for 10 s, 60°C for 30
151 s, 72°C for 40 s, and the final elongation at 72°C for 5 min. The PCR product was cleaned with a
152 1.8x bead solution and eluted in 40µL elution buffer to make the final library.

153 2.3 Sequencing, read processing and variant calling

154 The prepared library was sequenced using the 75bp PE v3 sequencing kit on an Illumia NextSeq.
155 Reads were aligned to the *P. alecto* reference genome ASM32557v1 (Zhang et al., 2013) from
156 GenBank using bwa mem 0.7.17-r1198-dirty (Li, 2013) with default settings. Using bcftools
157 1.19 (Danecek et al., 2021), a pileup was generated with a minimum base quality of 10 and
158 minimum mapping quality of 20 and variants were called. Invariant sites were included to inform
159 demographic modelling. The variant calls were split into two datasets for filtering and analysis:
160 an "all" set containing all four species (n=242) and an "*P. alecto* + *P. conspicillatus*" set
161 (n=150). Filtering was conducted separately for both datasets to minimize the number of SNPs
162 excluded due to missingness in species other than *P. alecto* and *P. conspicillatus*. Sites were
163 filtered using vcftools 0.1.16 (Danecek et al., 2011) by a minimum depth of 5, a minimum minor
164 allele frequency of 0.05, and a maximum missingness of 50% across all samples. Next, variants
165 were filtered to retain only biallelic SNPs. The low-quality 5bp flanking regions of all aligned

reads were also removed. PLINK2 2.00a2.3LM (Chang et al., 2015) was used to prune linked SNPs with "--indep-pairwise 50 5 0.3". Kinship coefficients were calculated using the KING algorithm (Manichaikul et al., 2010) as implemented in PLINK2. Heterozygosity per sample was also calculated using PLINK2.

2.4 Population genetic analysis

The "all" and "*P. alecto* + *P. conspicillatus*" datasets were interrogated independently using multiple population genetic analyses. For our more detailed population genetic investigation, the "*P. alecto* + *P. conspicillatus*" individuals were assigned to six geographic regions: Indonesia, North West Australia, North East Australia, East Australia, Wet Tropics Australia, and New Guinea (Figure S1). The Wet Tropics region of Queensland, Australia is a unique region of wet tropical forests and distinct from other sampled locations in North East Australia. Sampling coordinates were plotted on a map using the sf package (Pebesma, 2018). Distances between sampling coordinates were calculated using the distHaversine function of the R package geosphere 1.5 (https://github.com/rspatial/geosphere). Nucleotide diversity was assessed in non-overlapping 100kb windows using pixy 1.2.11.beta1 (Korunes & Samuk, 2021), removing windows with fewer than 50 sites. Pairwise genome-wide genetic differentiation (F_{ST}) for population pairs was calculated using stacks populations 2.52 (Rochette et al., 2019). Principal component analysis was carried out with SNPRelate 1.40.0 (Zheng et al., 2012). To detect admixture and potential hybridization, population structure was also inferred using fastStructure 1.0 (Raj et al., 2014) with 1 to 15 clusters and the default prior, using the provided chooseK method to select an optimal number of clusters that maximizes the log-marginal likelihood lower bound of the data. To validate potential hybridization inferred using principal component analysis (PCA) and admixture analysis, we selected ancestry-informative markers with a species-specific allele frequency of at least 0.85 and used them to generate triangle plots of hybrid index and interclass heterozygosity using triangulaR (Wiens & Colella, 2024). A phylogenetic tree was then inferred using RAxML 8.2.12 (Stamatakis, 2014) with the "GTRCAT" model to account for using only variant sites and 100 bootstraps. The Indonesian *P. alecto alecto* individuals were used as the outgroup.

2.5 Migration inference

Migrations between the six geographic populations of *P. alecto* and *P. conspicillatus* were firstly inferred using Treemix 1.13 (Pickrell & Pritchard, 2012) with the Indonesian *P. alecto alecto* individuals set as the outgroup. Treemix uses SNP-based allele frequency data to infer discrete migration events on a phylogenetic tree capturing population relationships.We ran Treemix with 500 SNPs per block for covariance matrix estimation and values of 0-7 migration edges m, with 10 replicates for each value of m. We then used the Evanno method implemented in the R package OptM to determine the optimal value of m (Fitak, 2021). In addition, we estimated the amount of variance in population relatedness explained by the Treemix graph model and used a threshold of 99.8% for selecting the number of migration edges (Pickrell & Pritchard, 2012), finding that both methods produced consistent results (m=3). To complement the Treemix analysis by also explicitly exploring spatial genetic structure, we applied FEEMSmix to calculate an effective migration surface on a geographic grid with a cell spacing of 220km (Shastry et al., 2025). FEEMSmix adds long-range migration to the FEEMS framework, which infers migration rates on the edges of a graph of connected nodes representing local populations. Cross-validation was used to identify the migration edge weight penalty, which was set to λ=2. We set the node-specific variance penalty to λ_q=1 and found 4 long-range migration edges to improve model fit.

To better model continuous gene flow across different time periods, we next investigated gene flow between and within the *P. alecto* and *P. conspicillatus* population using coalescent simulations based on the site frequency spectrum implemented in fastsimcoal2 2.8 (Excoffier et al., 2013). To avoid overlap between populations, three specimens from North West Australia (M53754, M54659, M54660) assigned to the Indonesian cluster by fastSTRUCTURE were excluded from this analysis. To account for the missing values in our ddRAD genotype set while generating a complete data matrix, we maximized the number of segregating sites by using a projection of samples based on EasySFS (https://github.com/isaacovercast/easySFS) which relies on methods implemented in dadi (Gutenkunst et al., 2009). The "--total-length" parameter was set based on the variant and the invariant sites detected in the aligned reads for each population pair. We defined four demographic scenarios for comparison between population pairs: strict isolation, ancient migration, recent migration, and constant migration. We allowed for asymmetric migration between populations. We assumed a mutation rate of 2.5×10^{-8} mutations

224 per nucleotide site per generation (Nachman & Crowell, 2000). This mutation rate, despite lower
225 mutation rates also estimated for *Myotis* bats (Ray et al., 2008), is thought to reflect the most
226 accurate mutation rate in mammals including bats (Sovic et al., 2016). We also assumed a
227 generation time of 4 years based on our observations in the field and on the literature (McIlwee
228 & Martin, 2014). To evaluate the demographic scenarios, we ran fastsimcoal2 for 100 replicates
229 per migration scenario using the parameters "-m -n 50000 -L 30 -M -C 10". After selecting the
230 replicate with the highest maximum composite likelihood for each scenario, we used the Akike
231 Information Criterion (AIC) to determine the best fitting migration scenario for each population
232 pair based on the highest AIC score. Next, to calculate confidence intervals for all model
233 parameter estimates, we ran 100 parametric bootstrap replicates by simulating site frequency
234 spectra from the estimates of each of the best-fitting models (Excoffier et al., 2013).

235 2.6 Bayesian divergence-time estimation

236 To investigate between-species divergence-times and validate parameters inferred with
237 fastsimcoal2, we used BEAST2 2.7.7 (Bouckaert et al., 2019) with the plugin SNAPP to infer
238 divergence-times based on SNPs (Stange et al., 2018). Three samples without inferred admixture
239 were selected based on genotype data completeness per species. Ascertainment bias correction to
240 adjust parameters based only on variable sites was used. A lognormal prior (real mean=3.54,
241 sd=0.3, offset=0) on the crown group containing *P. poliocephalus*, *P. alecto* and *P.*
242 *conspicillatus* was set to calibrate the analysis based on a previously inferred age of 3.54 mya
243 (Almeida et al., 2014). The moderately high standard deviation was selected to account for the
244 uncertainty inherent in secondary calibrations and to ensure overlap with other slightly deviating
245 estimates for the group (Tsang et al., 2020). Inference was run for over 40 million MCMC
246 generations with a 10% burn-in and convergence was confirmed using visual inspection in
247 Tracer 1.7.2 with a criterion of effective sample size (ESS) >200 for each parameter.

3 Results

3.1 Sequencing, read processing and variant calling

For each collected sample, an average of 2.14m paired reads of 43bp trimmed length were generated. The mean alignment rate to the *P. alecto* reference genome was 96.69%, covering an average of 4.31% of the genome (Table S2). A total of 2,421,904 raw variants were detected and then filtered for minimum allele depth, missingness per variant, minor allele frequency, and linkage disequilibrium (see Methods). For the "all" dataset (n=242), 18,762 filtered SNPs with an average per-sample depth of 11.50× were retained after filtering. For the "alecto + conspicillatus" dataset (n=150), 26,519 SNPs with an average per-sample depth of 11.16× were retained after filtering.

3.2 Population structure of four flying-fox species

We found a wide range of genome-wide diversity in the flying-fox species as measured by heterozygosity H (Figure S2) and nucleotide diversity π (Figure S3). Based on the genetic evidence, we split *P. alecto* into two groups for all analyses: the Indonesian subspecies group *P. alecto alecto* (n=9) and all other *P. alecto* individuals (n=86). These two groups are likely distinct species with similar morphology. We found intermediate diversity relative to the other species in *P. alecto* (mean H = 0.006, mean π = 0.008) and *P. conspicillatus* (mean H = 0.005, mean π = 0.008). *P. scapulatus* had the highest diversity (mean H = 0.007, mean π = 0.008) and *P. poliocephalus* the lowest (mean H = 0.004, mean π = 0.004). *P. alecto alecto* was an outlier with a uniformly low diversity across samples (mean H = 0.003, mean π = 0.003). Across the regional populations of *P. alecto* and *P. conspicillatus*, diversity within Australia showed limited variation, but the Indonesian *P. alecto* population and the New Guinean *P. conspicillatus* population showed lower diversity compared to Australian populations of the same species (Figure S2B and Figure S3B).

Across the four flying-fox species, we observed a wide range of between-species genetic differentiation, with F_{ST} ranging from 0.06 for *P. alecto* - *P. conspicillatus* to 0.28 for *P. scapulatus* - *P. alecto alecto* (Figure S4, Table S3). Within the closely related *P. alecto* - *P.*

conspicillatus group, F_{ST} values indicated low genetic differentiation between the New Guinean and the Australian *P. conspicillatus* (F_{ST}=0.02) but higher differentiation between the Indonesian and Australian *P. alecto* populations in (F_{ST}=0.05-0.07) (Figure S5, Table S4). Additionally, we found that the Indonesian *P. alecto* population was most differentiated from the New Guinean *P. conspicillatus* (F_{ST}=0.14) and less differentiated from the Australian *P. conspicillatus* (F_{ST}=0.12).

PCA delineated the samples by species, but suggested close genetic association between *P. alecto* and *P. conspicillatus* (Figure 2, Table S5). Additional PCA of the *P. alecto* and *P. conspicillatus* group showed limited population structure within *P. conspicillatus*. However, *P. alecto* individuals formed mostly discrete groups by country as well as showing some separation within Australia between North West Australia and the remaining groups in East Australia and North East Australia (Figure 2D, Table S6). Based on Bayesian population structure inference, the majority of Australian *P. alecto* individuals show signals of admixture, either from the Indonesian *P. alecto* cluster or from the *P. conspicillatus* cluster (Figure 2E). Multiple *P. alecto* individuals (samples 1702005, 1702029) and also *P. conspicillatus* individuals (samples 2811016, 1306014) show substantial admixture. For instance, with an admixture proportion of 48.5% from the *P. alecto* cluster, the *P. conspicillatus* sample 1306014 is likely a hybrid or backcross. Missingness can spuriously pull samples to the center in PCA (Yi & Latch, 2022), but the missingness of 25.1% in this sample is average for the population (mean=21.5%, sd=12.3%).

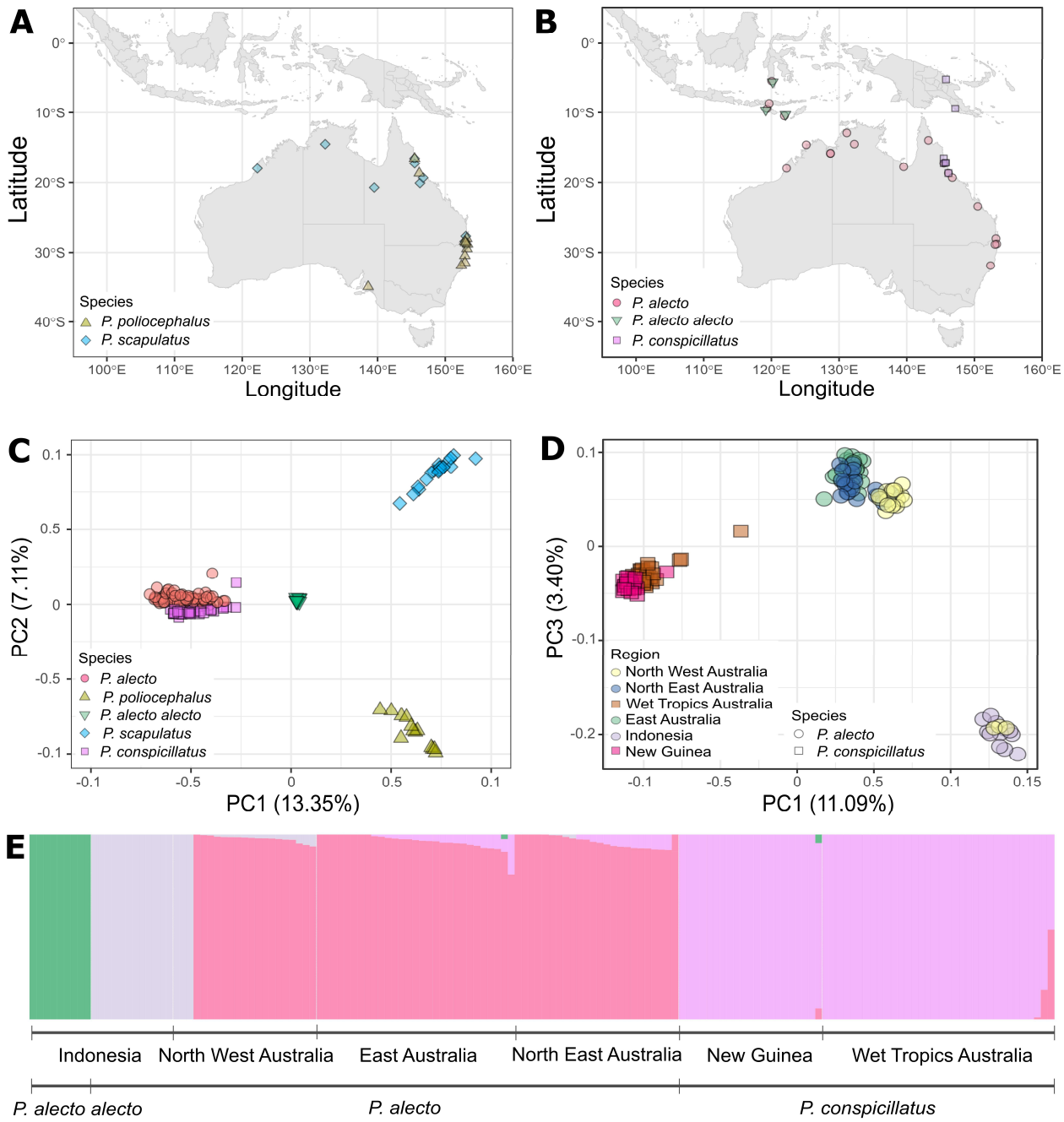

Figure 2. Population structure of four flying-fox species in Australia, Indonesia and New Guinea. A) Sampling locations for *Pteropus poliocephalus* and *P. scapulatus*. B) Sampling locations for *P. alecto* and *P. conspicillatus*. C) SNP-based principal component analysis (PCA) of all sampled species. The percentage of variance explained by each PC is shown on the axis. D) SNP-based PCA of six geographic populations of *P. alecto* and *P. conspicillatus*. The individual intermediate between the *P. conspicillatus* and the main Australian *P. alecto* cluster is sample 1306014. E) Structure plot of *P. alecto* and *P. conspicillatus* samples with four admixture groups. Bars indicate the proportion of each sample assigned to each group, revealing admixture between groups. The rightmost *P. conspicillatus* individual with 48.5% admixture from the *P. alecto* group is sample 1306014.

PCA and model-based population structure inference cannot readily distinguish admixture from isolation by distance and may thus not be sufficient to infer hybridization (Wiens & Colella, 2025). To complement these analyses and validate the signature of hybridization, we therefore calculated hybrid indices of all *P. alecto* and *P. conspicillatus* individuals, representing the proportion of ancestry received from each parental population based on a set of 36 ancestry-informative markers. The triangle plot based on hybrid index and interclass heterozygosity confirmed hybridization between the species, indicating that samples including 1306014, 1702005 and 1702012 are *P. alecto* × F1 backcrosses and sample 2811016 is a *P. conspicillatus* × F1 backcross (Figure 3). In addition, *P. alecto* samples 1610001, 1702029, and 1702028 were identified as later backcross generations. Overall, signatures of admixture from the *P. conspicillatus* cluster to the *P. alecto* cluster are more prevalent, with the majority of *P. conspicillatus* individuals not showing evidence of admixture or hybridization.

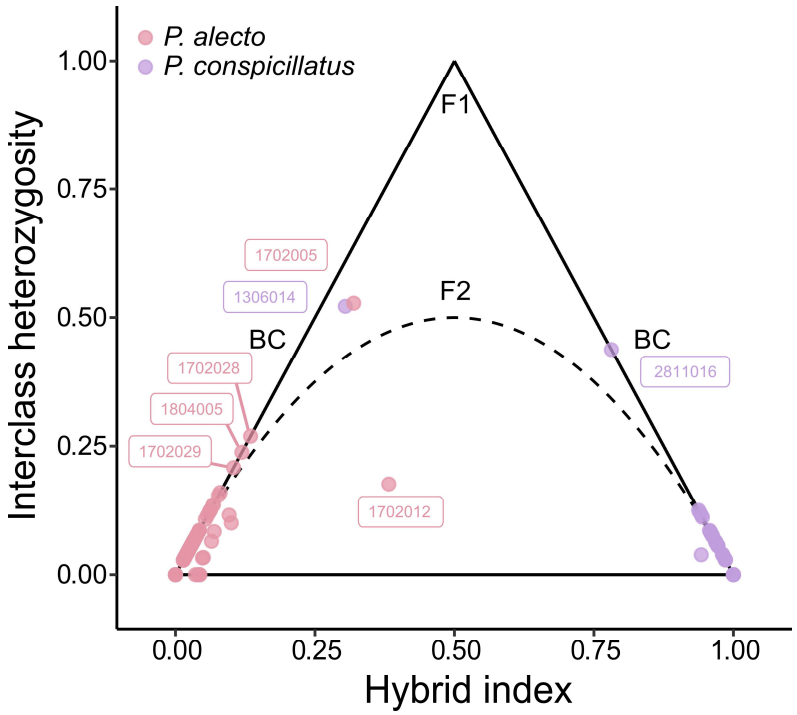

Figure 3. Triangle plot of admixture between *P. alecto* and *P. conspicillatus* based on 36 ancestry-informative SNP markers. The hybrid index of F_1 and F_2 hybrids is expected to be 0.5 while backcross (BC) individuals between hybrids and parental lineages are expected to lie on the edges of the triangle with elevated heterozygosity and hybrid indices.

A SNP-based maximum likelihood phylogeny of *P. alecto* and *P. conspicillatus* recovered robust (bootstrap support>70) clades grouping these two species as distinct from the outgroup, but none

322 of the six geographic groups formed robust clades (Figure S6). The *P. alecto* backcross sample
323 1702029 forms a sister clade to the robust clade containing of all other *P. alecto* and *P.*
324 *conspicillatus* individuals. The predominantly Indonesian *P. alecto* clade contains three
325 individuals (M54660, M53754, and M54659) sampled from North West Australia with robust
326 bootstrap support. The Australian *P. alecto* individuals do not form robust geographic clades,
327 although the clade containing all North West Australian individuals does not have any members
328 from the East Australian group suggesting some genetic separation. In contrast to *P. alecto* and
329 *P. conspicillatus*, *P. poliocephalus* and *P. scapulatus* showed no geographic structure across the
330 sampled populations (Figure S7).

331 3.3 Admixture occurs between *P. alecto* and *P. conspicillatus* populations 332 along a geographic ring

333 We next investigated population splits and admixture events in more depth using a maximum
334 likelihood approach to infer migration edges in a population tree and coalescent simulations
335 based on the site frequency spectrum to infer migration rates. We found support for three
336 migration edges connecting *P. conspicillatus* to *P. alecto* (Figure S8). Migration edge weight
337 decreased with geographic distance, showing lower migration between *P. conspicillatus* and the
338 more distant North West Australian population consistent with spatial patterns of admixture
339 (Figure 4A). The inferred effective migration surface emphasized high-levels of within-species
340 connectivity, including long-range migrations from East Australia to North West Australia and
341 from Indonesia and New Guinea to Australia (Figure 4B). Migration edges connecting New
342 Guinean *P. conspicillatus* to Indonesian *P. alecto* were weak.

343 To further probe patterns of gene flow between distant populations, we used coalescent
344 simulations to test multiple demographic scenarios including isolation and migration at three
345 different time scales. These coalescent simulations indicated recent migration after a period of
346 isolation and divergence between *P. conspicillatus* populations and all *P. alecto* populations,
347 forming a ring between Indonesia, Australia and New Guinea (Table 1 and Figure S8C).
348 Migration between Indonesian and Australian *P. alecto* populations was estimated to have
349 ceased 14 to 2,190 ya (Table S7). This is consistent with the evidence of migration between
350 Indonesia and North West Australia from the historical *P. alecto* collected from 1989 to 2003

(Figure 4A and Figure S6). Although we inferred migration connecting the chain of four *P. alecto* populations from Indonesia to East Australia, we also found that genetic relatedness decreased linearly with distance in this species (Figures 4C and 4D, Table S8). When considering pairwise comparisons of genetic and geographic distance for all *P. alecto* individuals, we found a strong, but not significant, effect (Mantel test, r=-0.51, *p*-value=1). Further investigation of the relationship between the genetic relatedness, captured by the kinship coefficient and geographic distance between individuals, revealed that the correlation between genetic and geographic distance was primarily driven by comparisons between Indonesian and Australian individuals (Figure 4D). Consistent with our population structure analyses, fastsimcoal2 estimates showed consistently higher migration from *P. conspicillatus* populations to *P. alecto* populations. One exception was the comparison of North East Australia and New Guinea, where we inferred a higher rate of migration from the admixed *P. alecto* population to New Guinean *P. conspicillatus*.

Divergence-times between *P. conspicillatus* and *P. alecto* were estimated by fastsimcoal2 using a fixed mammalian mutation rate to be between 60.5 thousand years ago (kya) to 83.4 kya, with a high estimate of 273.1 kya when comparing Indonesian *P. alecto* with New Guinean *P. conspicillatus* (Table S7). In broad agreement with these recent divergence-times, Bayesian species-level divergence-time inference using a calibration point from an earlier dated phylogeny found that *P. alecto* and *P. conspicillatus* diverged 323.4 kya (95% interval = 160.2-518.2 kya) (Figure S9).

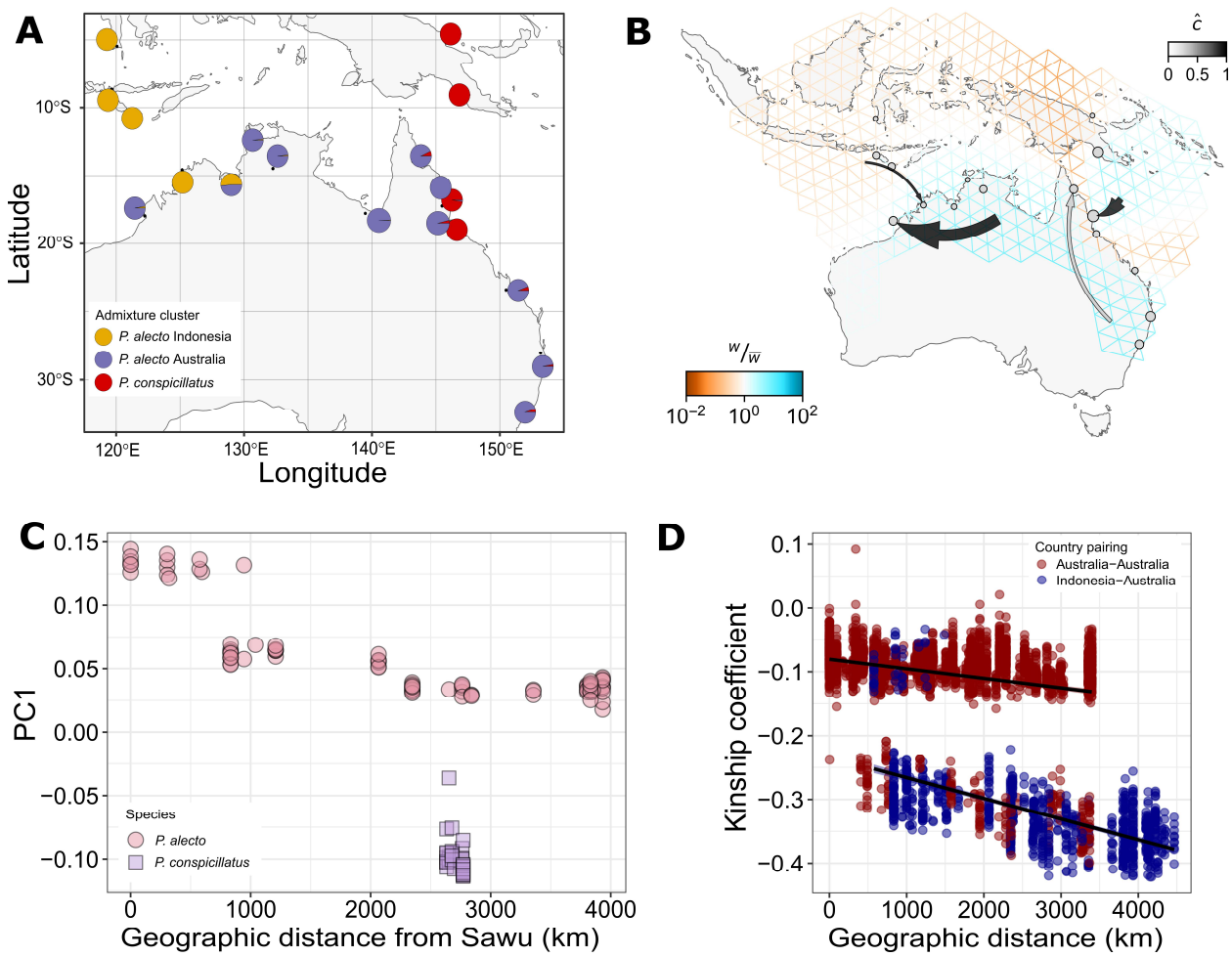

Figure 4. Gene flow in *Pteropus. alecto* and *P. conspicillatus* along a geographic ring ranging across Indonesia, Australia, and Papua New Guinea. A) Admixture proportions for local demes of *P. alecto* and *P. conspicillatus*. Admixture is inferred via fastSTRUCTURE using excluding *P. alecto alecto* from the result (see Figure 2E). B) Effective migration surface with long-range gene flow across the sampled distribution of *P. alecto* and *P. conspicillatus*. Weights (w) on the edges that represent migration rates between pairs of demes are shown relative to their mean value ($\underline{w}$) across all edges (Marcus et al., 2021). High migration regions are shown in blue and low migration regions in orange. Long-range migration edges are indicated by arrows, which decrease in size with each added long-range edge and are colored by the estimated source fraction ($\hat{c}$) (Shastry et al., 2025). C) Genetic differentiation is correlated with geographic distance in *P. alecto*. The first principal component (Table S6) is plotted against the geographic distance of each sample from Sawu, Indonesia, which is at one of the edges of the ring. D) Pairwise genetic relatedness in *P. alecto* based on kinship coefficient is negatively correlated with geographic distance in Indonesian-Australian sample pairs but less so in Australian-Australian pairs. Negative kinship coefficients indicate lower genetic relatedness in unrelated individuals.

386 **Table 1.** Inferred demographic parameters for four *P. alecto* (Indonesia, North West Australia, North East Australia, and East Australia) and two
387 *P. conspicillatus* (New Guinea and Wet Tropics Australia) populations based on coalescent simulation. Four migration scenarios (isolation,
388 ancient migration, recent migration, and constant migration) were compared based on the Akike Information Criterion (AIC). Years since
389 migration began are shown for recent migration and years since migration ended are shown for for ancient migration. Estimates shown were
390 selected from 100 replicates based on the likelihood. For additional inferred demographic parameters and 95% confidence intervals see Table S7.

Pop 1	Pop 2	Best migration scenario	Migration from Pop 2 to Pop 1	Migration from Pop 1 to Pop 2	Years since migration began/ended
New Guinea	Indonesia	recent	1.22×10^{-5}	3.14×10^{-5}	85,760
New Guinea	North West Australia	recent	5.23×10^{-5}	9.42×10^{-5}	11,456
New Guinea	North East Australia	recent	5.88×10^{-5}	1.26×10^{-4}	10,108
New Guinea	East Australia	recent	4.55×10^{-5}	9.22×10^{-5}	17,120
New Guinea	Wet Tropics Australia	constant	6.06×10^{-4}	1.80×10^{-4}	NA
Indonesia	North West Australia	ancient	1.29×10^{-4}	7.61×10^{-5}	1,116
Indonesia	North East Australia	ancient	1.18×10^{-4}	6.18×10^{-5}	996
Indonesia	East Australia	ancient	9.50×10^{-5}	5.12×10^{-5}	1,172
Indonesia	Wet Tropics Australia	recent	3.49×10^{-5}	2.36×10^{-5}	12,208
North West Australia	North East Australia	constant	3.99×10^{-4}	2.98×10^{-4}	NA
North West Australia	East Australia	recent	2.31×10^{-4}	3.43×10^{-4}	11,572
North West Australia	Wet Tropics Australia	recent	1.32×10^{-4}	1.07×10^{-4}	3,564
North East Australia	East Australia	ancient*	4.34×10^{-4}	3.82×10^{-4}	8
North East Australia	Wet Tropics Australia	recent	3.12×10^{-4}	1.86×10^{-4}	3,752
East Australia	Wet Tropics Australia	recent	1.70×10^{-4}	1.11×10^{-4}	7,220

391 * Inferred ancient migration ended so closely to recent time that it can reasonably be interpreted as constant migration.

4 Discussion

Our investigation of genome-wide SNPs across 242 flying-fox individuals from four species revealed panmictic weakly differentiated Australian populations and strong isolation-by-distance of Indonesian *P. alecto* populations but not New Guinean *P. conspicillatus* populations. Both *P. scapulatus* and *P. poliocephalus* show no evidence of population structure within Australia, consistent with their large populations (Macdonald et al., 2021; Vanderduys et al., 2024), higher mobility relative to *P. alecto* (Welbergen et al., 2020), and limited geographic barriers in their eastern Australian range. Interestingly, we found that the Indonesian *P. alecto alecto* subspecies (Andersen, 1912) forms a distinct lineage to the other *P. alecto* samples, diverging from other *P. alecto* and *P. conspicillatus* ca. 1.46 mya in a clear case of cryptic speciation. We expected higher genetic differentiation between disjunct *P. conspicillatus* populations, instead finding limited evidence for isolation between these populations based on summary statistics and coalescent modelling, suggesting that the roughly 150 km separating Australia and New Guinea does not represent a substantial geographic barrier for *P. conspicillatus*. Other flying-fox species including *P. vampyrus* and *P. niger* have also been shown to have limited population genetic structure and high connectivity between populations (Larsen et al., 2014; Tsang et al., 2018), though species such as *P. dasymallus* are known to exhibit isolation-by-distance between island populations (Chen et al., 2021). Such high levels of population connectivity across flying-foxes helps explain the high genome-wide heterozygosity, an important measure of genetic diversity, which we found in all four species. Indeed, *P. alecto* is known to harbor higher heterozygosity than other mammals (He et al., 2023; Zhang et al., 2013). Compared to genome-wide heterozygosity in a diverse set of mammals ranging from 0.012% in domestic cat to 0.16% in gorilla (Cho et al., 2013), our findings of heterozygosity of 0.55% in *P. alecto* and 0.68% in *P. scapulatus* suggest that flying-foxes may generally be outliers with higher genetic diversity than other mammals.

Overall, we found that the higher degree of genetic diversity in Australian flying-fox populations compared with other populations is not primarily a result of admixture with sympatric species, as has been suggested (Tsang, 2015), but of strong within-species gene flow across Australia. Nevertheless, we found evidence of moderate hybridization between *P. alecto* and *P.*

conspicillatus (Almeida et al., 2009). Consistent with hybridization rather than incomplete lineage sorting, admixed individuals primarily occurred in the broad region of distribution overlap in eastern Australia. However, hybrid backcross *P. alecto* individuals were not restricted to the narrow secondary contact zone with *P. conspicillatus* in the Wet Tropics region of Queensland, Australia. Instead, consistent with the high mobility of flying-foxes, hybrid backcrosses were widely distributed across eastern and northern Australia. We did not find any F_1 or F_2 hybrids and the modest number of substantially admixed individuals detected suggests that hybridization is ongoing but infrequent. Field observations indicate that the morphologically highly similar *P. alecto* and *P. conspicillatus* inhabit ecologically distinct niches, with *P. alecto* found in savanna woodland and rainforest (Palmer et al., 2000) and *P. conspicillatus* primarily in rainforest (Richards, 1990). Although more recent evidence suggests *P. conspicillatus* may not be a true rainforest specialist (Parsons et al., 2007), this divergence in ecological specialization may contribute to limiting gene flow between both species. These ecological niches may also have played a role in the initial divergence of these two species since niche conservatism can isolate diverging populations in distinct ranges during early allopatric speciation, but does not prevent secondary contact during later range shifts (Lin et al., 2025). Differences in habit choice may also contribute to the asymmetric gene flow, which is substantially higher from *P. conspicillatus* to *P. alecto*. If *P. alecto* is spreading into rainforest habitats occupied by *P. conspicillatus*, then such a range expansion can lead to asymmetric introgression of local genes into the genome of the encroaching species (Excoffier et al., 2009). Alternatively, asymmetric gene flow can also occur due to asymmetric mating between the sexes, as was found in two closely related horseshoe bat species (Mao et al., 2013). While *P. alecto* and *P. conspicillatus* do not differ substantially in size or morphology, asymmetric mating could still occur due to differences in mating behavior and timing.

We did not find conclusive evidence supporting our hypothesis that *P. alecto* and *P. conspicillatus* form an interbreeding population with gradual isolation-by-distance along the geographic ring connecting Australia, Indonesia, and New Guinea. Our findings that Australian populations of the two species interbreed and Indonesian *P. alecto* show strongest isolation-by-distance from New Guinean *P. conspicillatus* superficially supports the hypothesis of a ring species. Although the gene flow we infer between Australia and Indonesia depends on flying-foxes currently making a challenging journey of around 500 km in the present day, bats may use

452 reefs such as Ashmore reef and oil rigs as stepping stones. Historically, dispersal distances
453 during the Pleistocene have also been substantially lower as the Sahul Shelf extending from
454 Australia was exposed during periods of lower sea levels (Karin et al., 2020; Voris, 2000).
455 However, we did not sufficiently sample the hypothesized endpoint of the ring connecting
456 Indonesia to New Guinea to confirm that admixture ceased in this region. Additionally, the
457 substantial divergence between the species on the Australian mainland, despite limited
458 geographic barriers for such mobile animals, suggests that *P. alecto* and *P. conspicillatus* may
459 have diverged in allopatry on the islands of the Indo-Australian Archipelago and later colonized
460 Australia, establishing secondary contact and admixing. This scenario of allopatric speciation
461 and secondary contact is also supported by our coalescent modelling. Unfortunately, the
462 resolution of biogeographic analyses in flying-foxes is limited and only indicates *P. alecto* and *P.*
463 *conspicillatus* originated in the broad region of Australia, New Guinea and the South Pacific
464 (Tsang et al., 2020). Based on Bayesian divergence-time estimates, we found *P. alecto* and *P.*
465 *conspicillatus* diverged in the Pleistocene as recently as 369 kya. This time was shaped by
466 increases in land area and elevation in Wallacea (Hall, 2013) as well as the uplift of New Guinea
467 ca. 5 mya, which played a key role as an ecological "stepping stone" between Wallacea and the
468 Australian mainland (Roycroft et al., 2022). Notably, Australia and New Guinea were connected
469 at times of low sea level during the Pleistocene including up to ca. 8 kya (Dodson, 1989; Voris,
470 2000). During the Holocene, human-wildlife conflict (Preece, 2023) and the reduction of
471 rainforest habitat in Australia (Rule et al., 2012) may also have substantially impacted flying-fox
472 distributions. These geographic upheavals provided ample opportunities for speciation, but also
473 complicate reconstruction of flying-fox biogeography to establish the existence of a ring species.
474 Moreover, confirming a ring species requires strong evidence since seemingly clear cases of ring
475 species have been shown to result from more complex scenarios of vicariance, long-distance-
476 colonization and allopatry (Liebers et al., 2004). Extended sampling of the range of *P. alecto* and
477 *P. conspicillatus* outside of Australia could shed further light on the evolutionary origin of these
478 species.

479 Our findings also have implications for conservation management of flying-foxes and pathogen
480 control. *P. conspicillatus* is classified as endangered and hybridization, such as the cases we
481 identified with *P. alecto*, may increase extinction risk (Todesco et al., 2016). However, the
482 asymmetry of the gene flow between the two species, which results in limited admixture in *P.*

conspicillatus suggests that there is limited increased extinction risk due to hybridization. Furthermore, the constant migration inferred between New Guinea and Australian *P. conspicillatus* populations may increase the resilience of the species by maintaining diversity. Unlike *P. conspicillatus*, *P. alecto* is currently listed as "Least Concern" by the International Union for Conservation of Nature (IUCN) across its range. However, the cryptic species *P. alecto alecto* identified here may be at risk, particularly since Indonesian populations in Sulawesi have declined due to hunting pressure since the 1970s (Sheherazade & Tsang, 2015). Our population genetic findings of high connectivity between flying-fox populations, including across international borders, can also inform studies of pathogen transmission and the management of biosecurity risk (Breed et al., 2010). For example, *P. alecto* has been implicated as a reservoir for bat-borne pathogens including Hendra virus (Edson et al., 2019). The high migration rates we inferred between *P. alecto* populations suggests that emerging viral strains can rapidly spread across the wide distribution of its host. Although these risks are well-understood and mitigated between Australia and New Guinea, our study suggests that transmission between northern Australia and Indonesia is underappreciated. Additionally, hybridization between flying-foxes has also been suggested to explain the wide distribution of Nipah virus through interspecies viral transmission (Olival et al., 2020), implying pathogens hosted by *P. alecto* may readily be transmitted and spread by *P. conspicillatus*.

5 Conclusion

We have used genomic markers to provide new insights into the evolutionary history and population dynamics of flying-foxes, revealing high genetic connectivity across Australian populations, cryptic speciation within *P. alecto*, and high gene flow across disjunct *P. conspicillatus* populations in Australia and New Guinea. The isolation-by-distance observed in Indonesian *P. alecto* contrasts with the weak differentiation across large distances in other populations, highlighting the role of water barriers in shaping genetic structure. While our results do not support a ring species model for *P. alecto* and *P. conspicillatus*, they suggest a complex history of isolation-by-distance and admixture contributing to the evolution of these extremely recently diverged species.

6 Data and code availability

Raw sequence reads and metadata are deposited in the SRA (BioProject PRJNA1230740). All code used for the population genetic analysis and generation of figures is available via github (https://github.com/ascheben/pteropus_popgen_analysis).

7 Author contributions

AS: formal analysis, data curation, writing - original draft. **AMcK**: resources, data curation, validation, writing - review and editing. **TW**: resources, data curation, validation, writing - review and editing. **DAW**: conceptualisation, methodology, validation, writing - review and editing, supervision. **SSM**: investigation, writing - review and editing. **EPV**: resources, validation, writing - review and editing. **BLW**: conceptualisation, methodology, validation, writing - review and editing, supervision, funding acquisition.

8 Acknowledgements

This work was funded by the CSIRO Biodiversity, Ecosystem Knowledge and Services Program. We thank Owain Edwards for intellectual input and Samia Elfekih and Ian Cresswell for logistical support. We thank Tolga Bat Hospital, Bat Care Capricornia, Kimberly Wildlife Carers, Western Australian Museum, Port Moresby Botanical Gardens, National Flying-fox monitoring program (NFFMP), Cecelia Sanchez, Chris Todd &Wayne Boardman for assistance in collecting samples. We also thank Christina DeDora and Jesse Ingram for manuscript editing support.

9 Conflicts of interest

The authors declare no conflicts of interest.

10 Supplementary figures

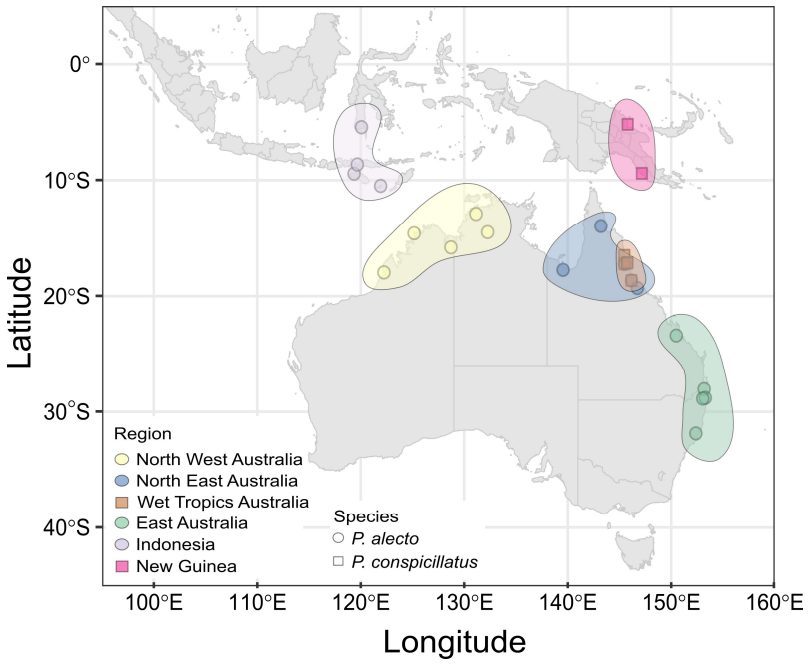

Figure S1. Roost locations and their assignment to distinct geographic regions sampled in this study. To highlight the regions relevant to this study, sampling locations here are shown only for the most widely distributed species *Pteropus alecto* and *P. conspicillatus*.

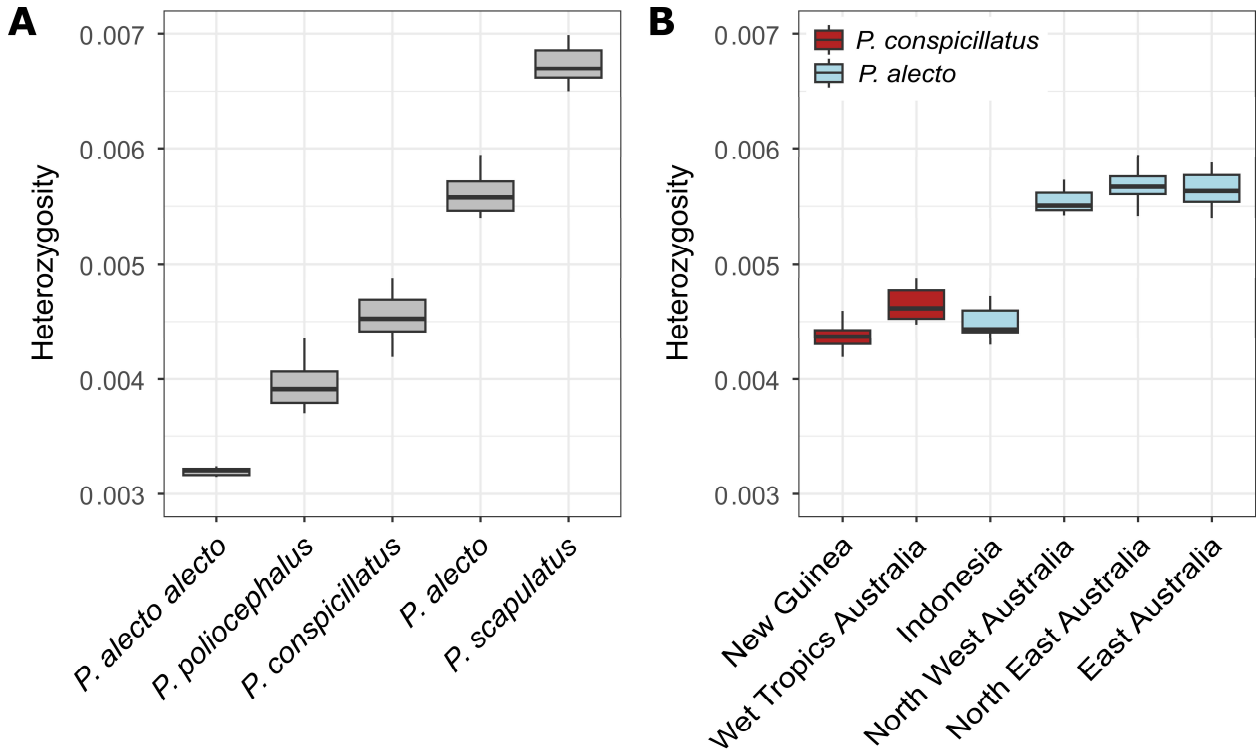

537 **Figure S2**. Genome-wide heterozygosity estimates for A) four flying-fox species and B) six regional
538 populations of *Pteropus alecto* and *P. conspicillatus*.

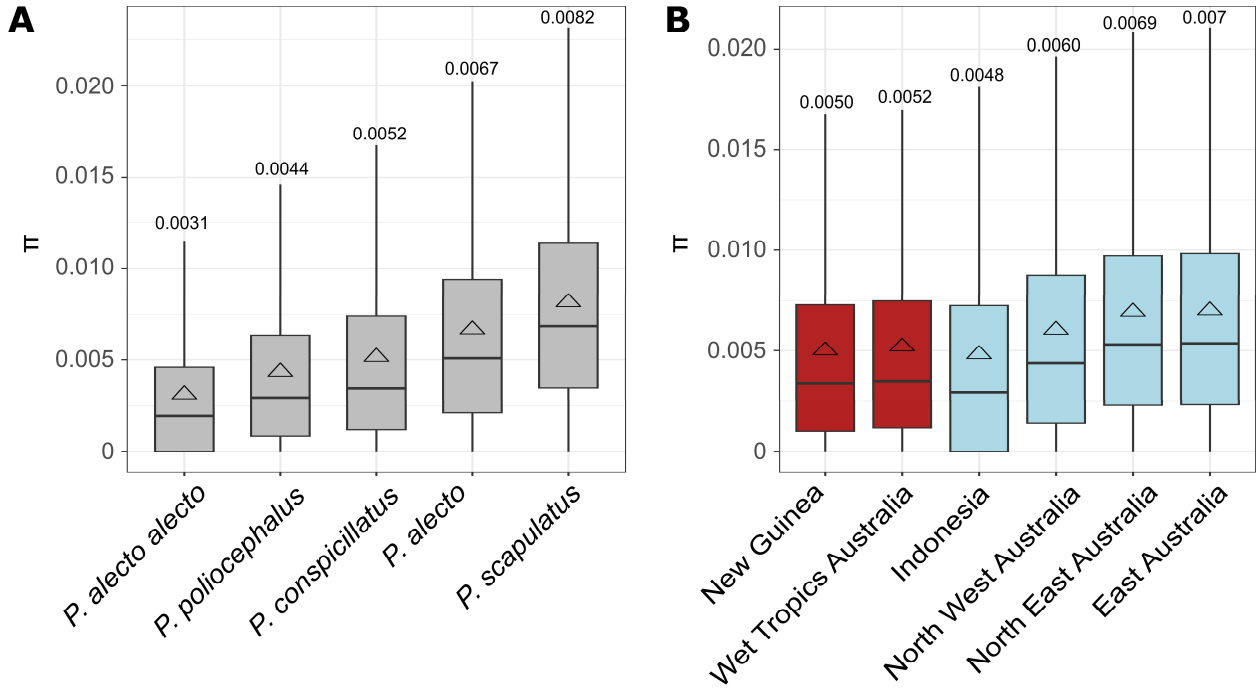

539 **Figure S3**. Genome-wide nucleotide diversity (π) estimates for A) four flying-fox species and B) six
540 regional populations of *Pteropus. alecto* and *P. conspicillatus*. Means are shown as triangles and specific
541 mean values are shown above each boxplot.

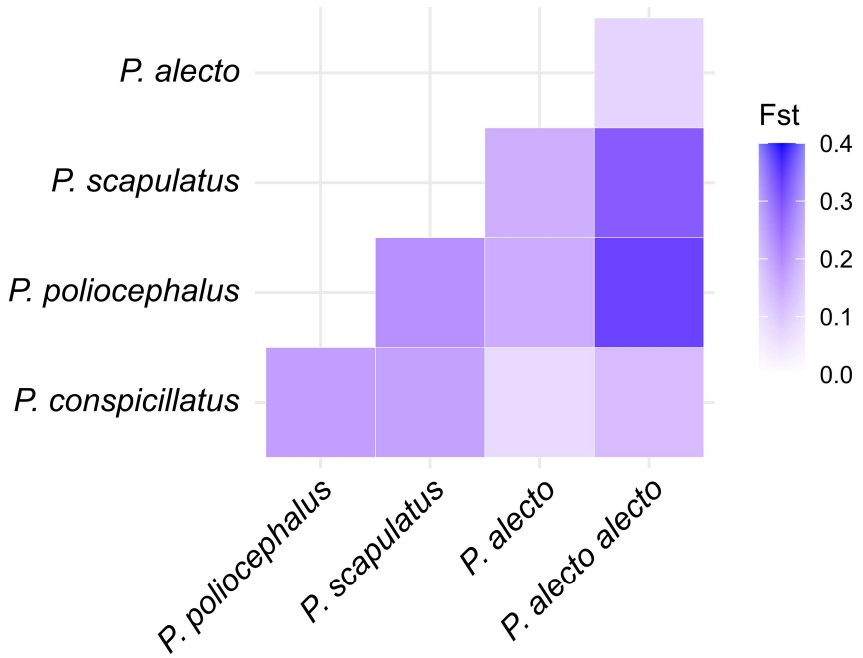

Figure S4. Genetic differentiation between four flying-fox species based on F_{ST}. The genetically distinct Indonesian *P. alecto alecto* group is shown separately.

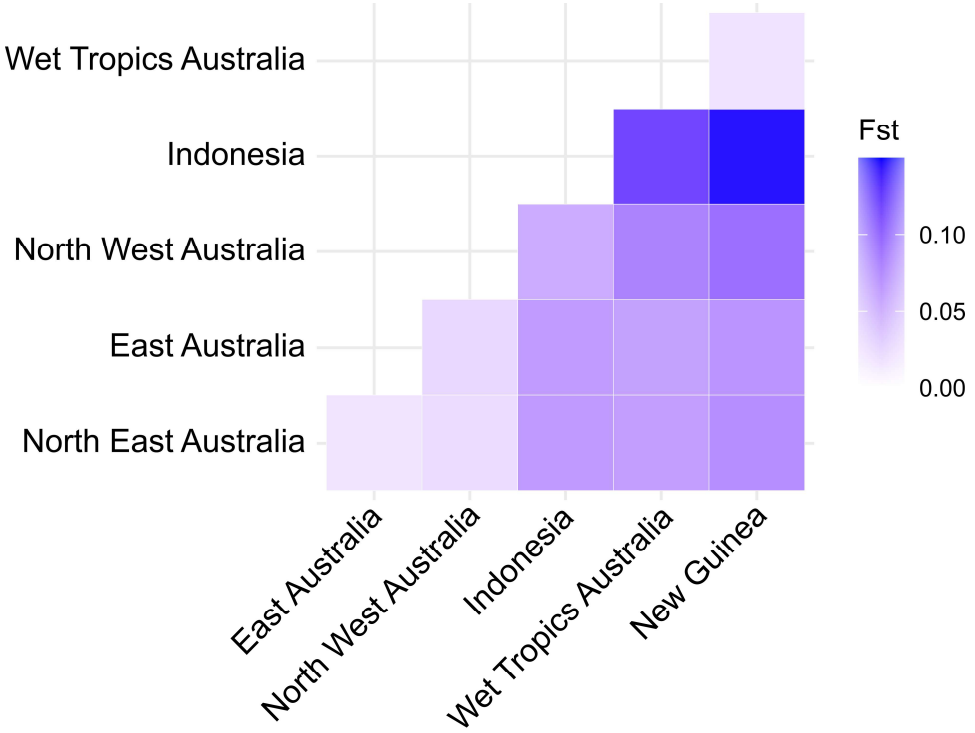

Figure S5. Genetic differentiation between geographic populations of *P. alecto* and *P. conspicillatus*. The Wet Tropics Australia and New Guinea groups represent *P. conspicillatus* and the other groups represent *P. alecto*.

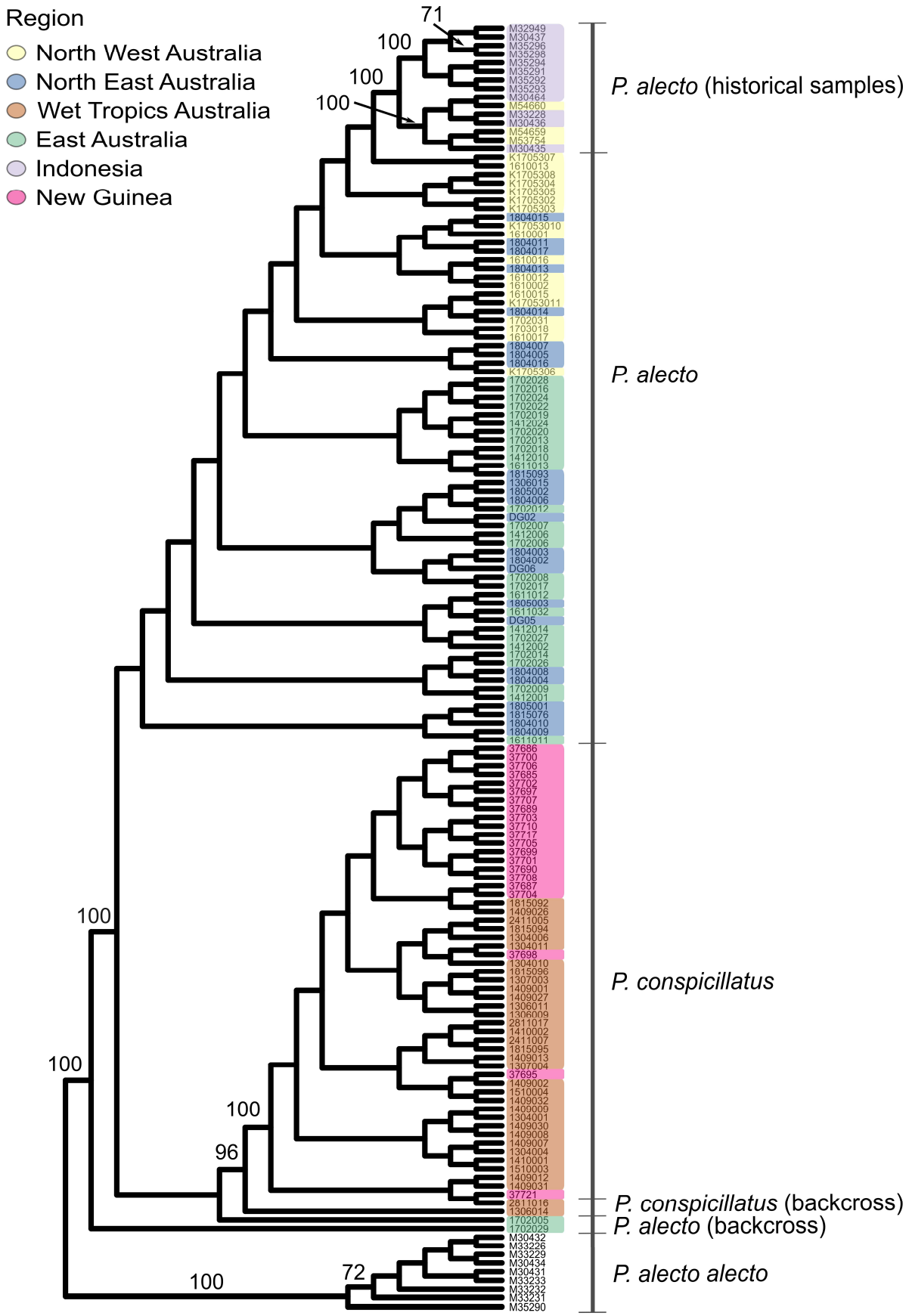
Region
North West Australia
North East Australia
Wet Tropics Australia
East Australia
Indonesia
New Guinea
71
100
100
100
100
100
100
96
100
72
P. alecto (historical samples)
P. alecto
P. conspicillatus
P. conspicillatus (backcross)
P. alecto (backcross)
P. alecto alecto

547

Figure S6. SNP-based maximum likelihood phylogeny of *Pteropus alecto* and *P. conspicillatus*. Individuals are highlighted in a color by geographic region and the Indonesian *P. alecto alecto* group is used as the outgroup. Historical *P. alecto* samples were collected from 1989 to 2003 (see Table S1). Bootstrap support values >70 are shown, highlighting robustly supported branches.

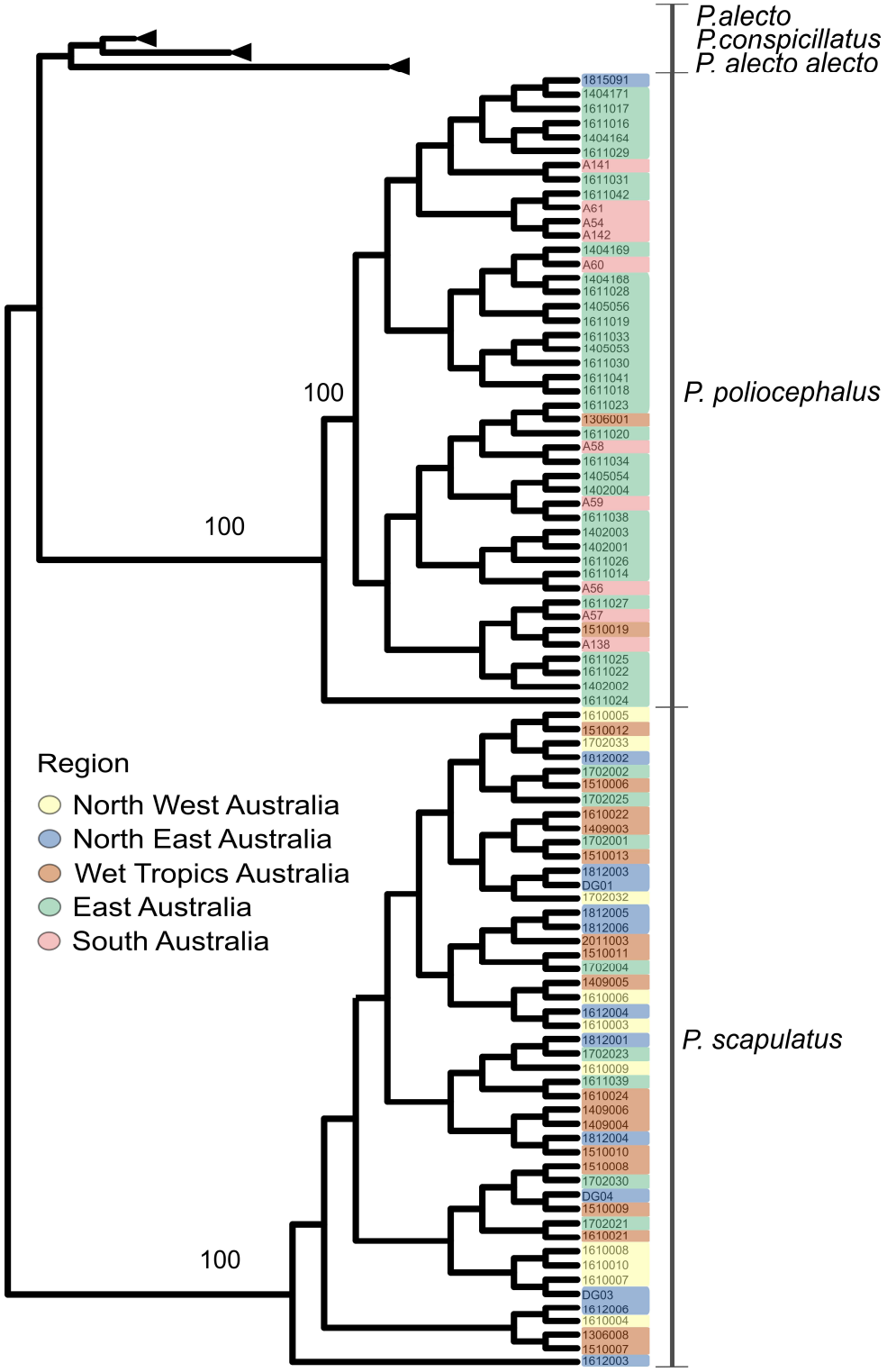

Figure S7. SNP-based maximum likelihood phylogeny of *Pteropus poliocephalus* and *P. scapulatus*. Individuals are highlighted in a color by geographic region. Bootstrap support values >70 are shown, highlighting robustly supported branches.

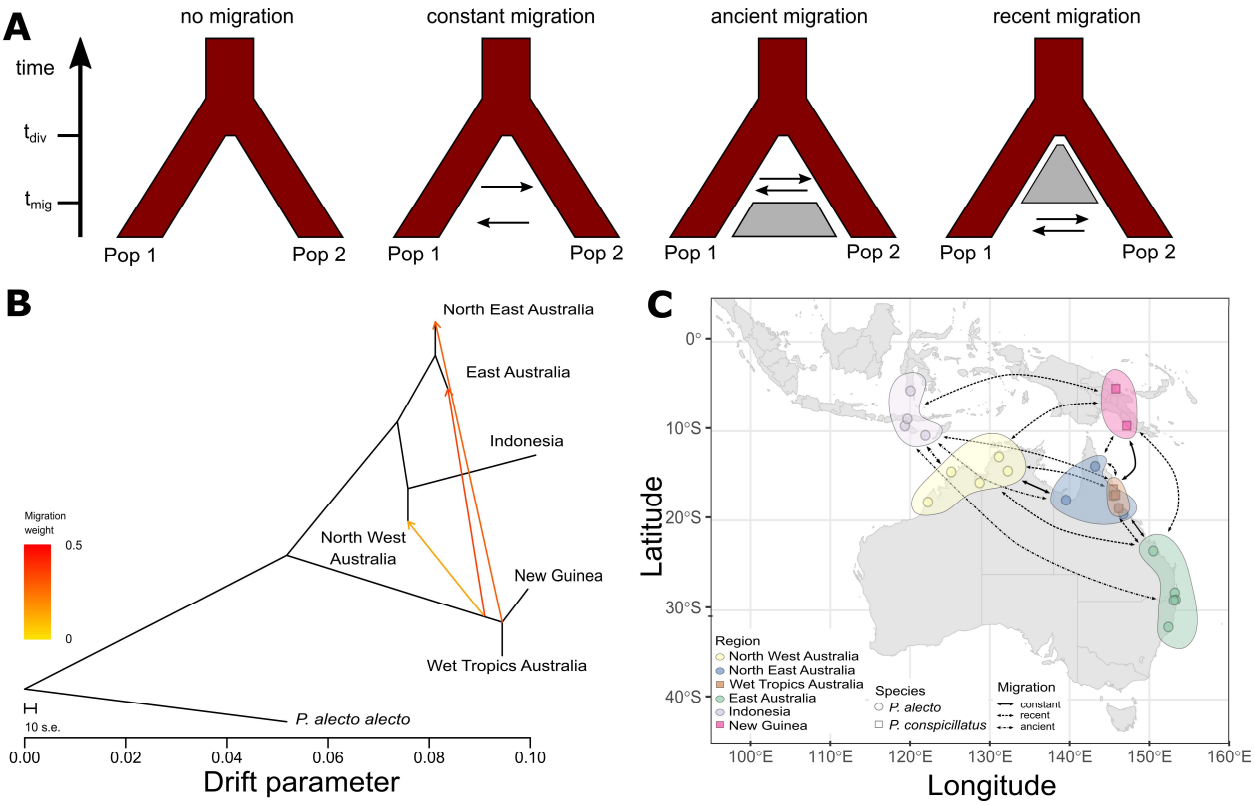

Figure S8. Gene flow in *Pteropus alecto* and *P. conspicillatus* along a geographic ring ranging across Indonesia, Australia and Papua New Guinea. A) Migration models for pairwise demographic histories between populations. Each model includes a parameter for the time that populations split (t_{div}) and models with non-constant migration include a parameter for the time that migration began or ceased (t_{mig}) depending on whether the migration occurred recently or in the past. Grey boxes indicate barriers to gene flow. B) Maximum likelihood tree with migration edges for six *P. alecto* and *P. conspicillatus* populations. *P. conspicillatus* populations include New Guinea and Wet Tropics Australia, the remainder are *P. alecto* populations. The Indonesian *P. alecto alecto* was used as the outgroup. C). Map of inferred migration scenarios between populations using coalescent simulations. Only recent and constant migrations are shown (see Table 1 for additional inferred parameters).

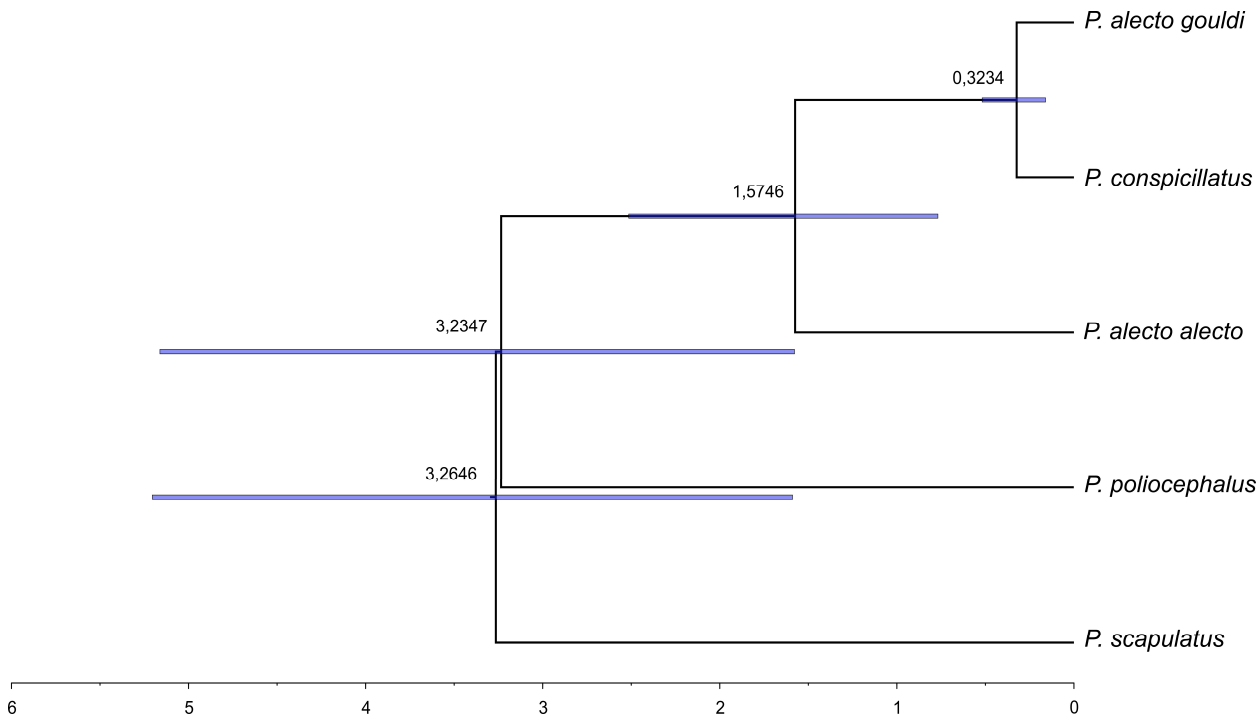

Figure S9. Dated phylogeny of sampled flying-fox species inferred using BEAST and SNAPP from genome-wide SNPs for three samples per branch. Mean divergence estimates per node are ages in millions of years before present. Blue bars show the 95% highest posterior density interval for each node. The subspecies designation *Pteropus alecto gouldi*, used to describe Australian *P. alecto*, is used here to indicate that the three sampled individuals for this branch all originate from Australia.

11 References

Abbott, R., Albach, D., Ansell, S., Arntzen, J. W., Baird, S. J. E., Bierne, N., Boughman, J., Brelsford, A., Buerkle, C. A., Buggs, R., Butlin, R. K., Dieckmann, U., Eroukhmanoff, F., Grill, A., Cahan, S. H., Hermansen, J. S., Hewitt, G., Hudson, A. G., Jiggins, C., … Zinner, D. (2013). Hybridization and speciation. *Journal of Evolutionary Biology*, *26*(2), 229–246. https://doi.org/10.1111/j.1420-9101.2012.02599.x

Aguillon, S. M., Fitzpatrick, J. W., Bowman, R., Schoech, S. J., Clark, A. G., Coop, G., & Chen, N. (2017). Deconstructing isolation-by-distance: The genomic consequences of limited dispersal. *PLoS Genetics*, *13*(8), e1006911. https://doi.org/10.1371/journal.pgen.1006911

Almeida, F. C., Simmons, N. B. & Giannini, N. P. (2020). A species-level phylogeny of Old World fruit bats with a new higher-level classification of the family Pteropodidae. *American Museum Novitates*, 3950, 1–24. https://doi.org/10.1206/3950.1

Almeida, F. C., Giannini, N. P., DeSalle, R., & Simmons, N. B. (2009). The phylogenetic relationships of cynopterine fruit bats (Chiroptera: Pteropodidae: Cynopterinae). *Molecular Phylogenetics and Evolution*, *53*(3), 772–783. https://doi.org/10.1016/j.ympev.2009.07.035

Almeida, F. C., Giannini, N. P., Simmons, N. B., & Helgen, K. M. (2014). Each flying fox on its own branch: A phylogenetic tree for *Pteropus* and related genera (Chiroptera: Pteropodidae). *Molecular Phylogenetics and Evolution*, *77*, 83–95. https://doi.org/10.1016/j.ympev.2014.03.009

Andersen, K. (1912). Catalogue of the Chiroptera in the collection of the British Museum. Volume I: Megachiroptera. British Museum (Natural History), London.

Bouckaert, R., Vaughan, T. G., Barido-Sottani, J., Duchêne, S., Fourment, M., Gavryushkina, A., Heled, J., Jones, G., Kühnert, D., Maio, N. D., Matschiner, M., Mendes, F. K., Müller, N. F., Ogilvie, H. A., Plessis, L. du, Popinga, A., Rambaut, A., Rasmussen, D., Siveroni, I., … Drummond, A. J. (2019). BEAST 2.5: An advanced software platform for Bayesian evolutionary analysis. *PLoS Computational Biology*, *15*(4), e1006650. https://doi.org/10.1371/journal.pcbi.1006650

Breed, A. C., Field, H. E., Smith, C. S., Edmonston, J., & Meers, J. (2010). Bats without borders: long-distance movements and implications for disease risk management. *Ecohealth*, *7*(2), 204–212. https://doi.org/10.1007/s10393-010-0332-z

Bruxaux, J., Zhao, W., Hall, D., Curtu, A. L., Androsiuk, P., Drouzas, A. D., Gailing, O., Konrad, H., Sullivan, A. R., Semerikov, V., & Wang, X.-R. (2024). Scots pine—Panmixia and the elusive signal of genetic adaptation. *The New Phytologist*, *243*(3), 1231–1246. https://doi.org/10.1111/nph.19563

Chang, C. C., Chow, C. C., Tellier, L. C., Vattikuti, S., Purcell, S. M., & Lee, J. J. (2015). Second-generation PLINK: Rising to the challenge of larger and richer datasets. *GigaScience*, *4*(1), s13742-015-0047–0048. https://doi.org/10.1186/s13742-015-0047-8

Chen, S.-F., Juan, C.-H., Rossiter, S. J., Kinjo, T., Fukui, D., Kawai, K., Tsang, S. M., Veluz, M. J., Sakurai, H., Lin, H.-C., Jang-Liaw, N.-H., Osawa, K., Ko, W.-Y., & Izawa, M. (2021). Population genetic structure of the insular Ryukyu flying fox *Pteropus dasymallus*. *Biotropica*, *53*(2), 548–559. https://doi.org/10.1111/btp.12897

Cho, Y. S., Hu, L., Hou, H., Lee, H., Xu, J., Kwon, S., Oh, S., Kim, H.-M., Jho, S., Kim, S., Shin, Y.-A., Kim, B. C., Kim, H., Kim, C., Luo, S.-J., Johnson, W. E., Koepfli, K.-P., Schmidt-Küntzel, A., Turner, J. A., … Bhak, J. (2013). The tiger genome and comparative analysis with lion and snow leopard genomes. *Nature Communications*, *4*(1), 2433. https://doi.org/10.1038/ncomms3433

Danecek, P., Auton, A., Abecasis, G., Albers, C. A., Banks, E., DePristo, M. A., Handsaker, R. E., Lunter, G., Marth, G. T., Sherry, S. T., McVean, G., & Durbin, R. (2011). The variant call format and VCFtools. *Bioinformatics*, *27*(15), 2156–2158. https://doi.org/10.1093/bioinformatics/btr330

Danecek, P., Bonfield, J. K., Liddle, J., Marshall, J., Ohan, V., Pollard, M. O., Whitwham, A., Keane, T., McCarthy, S. A., Davies, R. M., & Li, H. (2021). Twelve years of SAMtools and BCFtools. *GigaScience*, *10*(2), giab008. https://doi.org/10.1093/gigascience/giab008

Dodson, J. R. (1989). Late pleistocene vegetation and environmental shifts in Australia and their bearing on faunal extinctions. *Journal of Archaeological Science*, *16*(2), 207–217. https://doi.org/10.1016/0305-4403(89)90066-6

Eby, P. (1991). Seasonal movements of grey-headed flying-foxes, *Pteropus poliocephalus* (Chiroptera: Pteropodidae), from two maternity camps in northern New South Wales. *Wildlife Research*, *18*(5), 547–559. https://doi.org/10.1071/wr9910547

Edson, D., Peel, A. J., Huth, L., Mayer, D. G., Vidgen, M. E., McMichael, L., Broos, A., Melville, D., Kristoffersen, J., Jong, C. de, McLaughlin, A., & Field, H. E. (2019). Time of year, age class and body condition predict Hendra virus infection in Australian black flying foxes (*Pteropus alecto*). *Epidemiology & Infection*, *147*, e240. https://doi.org/10.1017/S0950268819001237

Excoffier, L., Dupanloup, I., Huerta-Sánchez, E., Sousa, V. C., & Foll, M. (2013). Robust demographic inference from genomic and SNP data. *PLoS Genetics*, *9*(10), e1003905. https://doi.org/10.1371/journal.pgen.1003905

Excoffier, L., Foll, M., & Petit, R. J. (2009). Genetic consequences of range expansions. *Annual Review of Ecology, Evolution, and Systematics*, *40*, 481–501. https://doi.org/10.1146/annurev.ecolsys.39.110707.173414

Fitak, R. R. (2021). OptM: Estimating the optimal number of migration edges on population trees using Treemix. *Biology Methods and Protocols*, *6*(1), bpab017. https://doi.org/10.1093/biomethods/bpab017

Fox, S. (2006). Population structure in the spectacled flying fox, *Pteropus conspicillatus*: A study of genetic and demographic factors. PhD thesis, James Cook University. https://researchonline.jcu.edu.au/8053/

Gutenkunst, R. N., Hernandez, R. D., Williamson, S. H., & Bustamante, C. D. (2009). Inferring the joint demographic history of multiple populations from multidimensional SNP frequency data. *PLoS Genetics*, *5*(10), e1000695. https://doi.org/10.1371/journal.pgen.1000695

Hall, R. (2013). The palaeogeography of Sundaland and Wallacea since the Late Jurassic. *Journal of Limnology*, *72*(s2). https://doi.org/10.4081/jlimnol.2013.s2.e1

He, H., Yang, H., Foo, R., Chan, W., Zhu, F., Liu, Y., Zhou, X., Ma, L., Wang, L.-F., & Zhai, W. (2023). Population genomic analysis reveals distinct demographics and recent adaptation in the black flying fox (*Pteropus alecto*). *Journal of Genetics and Genomics*, *50*(8), 554–562. https://doi.org/10.1016/j.jgg.2023.05.002

Irwin, D. E., Bensch, S., Irwin, J. H., & Price, T. D. (2005). Speciation by distance in a ring species. *Science*, *307*(5708), 414–416. https://doi.org/10.1126/science.1105201

Karin, B. R., Stubbs, A. L., Arifin, U., Iskandar, D. T., Arida, E., Austin, C. C., & McGuire, J. A. (2020). Crossing Lydekker's line: Northern Water Dragons (*Tropicagama temporalis*) colonized the Mollucan Islands of Indonesia from New Guinea. *Herpetologica*, *76*(3), 344–350. https://doi.org/10.1655/Herpetologica-D-19-00033

Korunes, K. L., & Samuk, K. (2021). pixy: Unbiased estimation of nucleotide diversity and divergence in the presence of missing data. *Molecular Ecology Resources*, *21*(4), 1359–1368. https://doi.org/10.1111/1755-0998.13326

Larsen, P. A., Hayes, C. E., Wilkins, M. A., Gomard, Y., Sookhareea, R., Yoder, A. D., & Goodman, S. M. (2014). Population genetics of the Mauritian flying fox, *Pteropus niger*. *Acta Chiropterologica*, *16*(2), 293–300. https://doi.org/10.3161/150811014X687251

Li, H. (2013). Aligning sequence reads, clone sequences and assembly contigs with BWA-MEM. *arXiv*. https://doi.org/10.48550/arXiv.1303.3997

Liebers, D., de Knijff, P., & Helbig, A. J. (2004). The herring gull complex is not a ring species. *Proceedings of the Royal Society B: Biological Sciences*, *271*(1542), 893–901. https://doi.org/10.1098/rspb.2004.2679

Lin, T.-H., Shen, Z.-Y., Chou, M.-H., Sun, P.-W., Shen, C.-C., Huang, J.-P., & Lin, S.-M. (2025). Allopatric speciation and interspecific gene flow driven by niche conservatism of *Diploderma* tree lizards in Taiwan. *Molecular Ecology*, e17718. https://doi.org/10.1111/mec.17718

Lomolino, M. V. (2000). A call for a new paradigm of island biogeography. *Global Ecology and Biogeography*, *9*(1), 1–6. https://doi.org/10.1046/j.1365-2699.2000.00185.x

Macdonald, S. L., Bradford, M., McKeown, A., Vanderduys, E., Hoskins, A., & Westcott, D. (2021). Camp site habitat preferences of the little red flying-fox (*Pteropus scapulatus*) in Queensland. *Australian Journal of Zoology*,*68*, 234–253. https://doi.org/10.1071/ZO20079

Manichaikul, A., Mychaleckyj, J. C., Rich, S. S., Daly, K., Sale, M., & Chen, W.-M. (2010). Robust relationship inference in genome-wide association studies. *Bioinformatics*, *26*(22), 2867–2873. https://doi.org/10.1093/bioinformatics/btq559

Mao, X., Thong, V. D., Bates, P. J. J., Jones, G., Zhang, S., & Rossiter, S. J. (2013). Multiple cases of asymmetric introgression among horseshoe bats detected by phylogenetic conflicts across loci. *Biological Journal of the Linnean Society*, *110*(2), 346–361. https://doi.org/10.1111/bij.12138

Marcus, J., Ha, W., Barber, R. F., & Novembre, J. (2021). Fast and flexible estimation of effective migration surfaces. *eLife*, *10*, e61927. https://doi.org/10.7554/eLife.61927

McIlwee, A. P., & Martin, L. (2014). On the intrinsic capacity for increase of Australian flying-foxes (*Pteropus* spp., Megachiroptera). *Australian Zoologist*, *32*(1), 76–100. https://doi.org/10.7882/AZ.2002.008

Nachman, M. W., & Crowell, S. L. (2000). Estimate of the mutation rate per nucleotide in humans. *Genetics*, *156*(1), 297–304. https://doi.org/10.1093/genetics/156.1.297

Neaves, L. E., Danks, M., Lott, M. J., Dennison, S., Frankham, G. J., King, A., Eldridge, M. D. B., Johnson, R. N., & Divljan, A. (2018). Unmasking the complexity of species identification in Australasian flying-foxes. *PLoS One*, *13*(4), e0194908. https://doi.org/10.1371/journal.pone.0194908

Neethling, M., Matthee, C. A., Bowie, R. C., & von der Heyden, S. (2008). Evidence for panmixia despite barriers to gene flow in the southern African endemic, *Caffrogobius caffer* (Teleostei: Gobiidae). *BMC Evolutionary Biology*, *8*(1), 325. https://doi.org/10.1186/1471-2148-8-325

O'Brien, J., Mariani, C., Olson, L., Russell, A. L., Say, L., Yoder, A. D., & Hayden, T. J. (2009). Multiple colonisations of the western Indian Ocean by *Pteropus* fruit bats (Megachiroptera: Pteropodidae): The furthest islands were colonised first. *Molecular Phylogenetics and Evolution*, *51*(2), 294–303. https://doi.org/10.1016/j.ympev.2009.02.010

Olival, K. J., Latinne, A., Islam, A., Epstein, J. H., Hersch, R., Engstrand, R. C., Gurley, E. S., Amato, G., Luby, S. P., & Daszak, P. (2020). Population genetics of fruit bat reservoir informs the dynamics, distribution and diversity of Nipah virus. *Molecular Ecology*, *29*(5), 970–985. https://doi.org/10.1111/mec.15288

Palmer, C., Price, O., & Bach, C. (2000). Foraging ecology of the black flying fox (*Pteropus alecto*) in the seasonal tropics of the Northern Territory, Australia. *Wildlife Research*, *27*(2), 169–178. https://doi.org/10.1071/wr97126

Parsons, J. G., Cairns, A., Johnson, C. N., Robson, S. K. A., Shilton, L. A., & Westcott, D. A. (2007). Dietary variation in spectacled flying foxes (*Pteropus conspicillatus*) of the Australian Wet Tropics. *Australian Journal of Zoology*, *54*(6), 417–428. https://doi.org/10.1071/ZO06092

Pebesma, E. (2018). Simple features for R: Standardized support for spatial vector data. *The R Journal*. https://digitalcommons.unl.edu/r-journal/626

Peel, A. J., Sargan, D. R., Baker, K. S., Hayman, D. T. S., Barr, J. A., Crameri, G., Suu-Ire, R., Broder, C. C., Lembo, T., Wang, L.-F., Fooks, A. R., Rossiter, S. J., Wood, J. L. N., & Cunningham, A. A. (2013). Continent-wide panmixia of an African fruit bat facilitates transmission of potentially zoonotic viruses. *Nature Communications*, *4*(1), 2770. https://doi.org/10.1038/ncomms3770

Pickrell, J. K., & Pritchard, J. K. (2012). Inference of population splits and mixtures from genome-wide allele frequency data. *PLoS Genetics*, *8*(11), e1002967. https://doi.org/10.1371/journal.pgen.1002967

Preece, N. (2023). Spectacled Flying-fox conflicts—Tucker, totem, taunt and threat. *Integrative Conservation*, *2*(3), 112–118. https://doi.org/10.1002/inc3.26

Raj, A., Stephens, M., & Pritchard, J. K. (2014). fastSTRUCTURE: Variational inference of population structure in large SNP data sets. *Genetics*, *197*(2), 573–589. https://doi.org/10.1534/genetics.114.164350

Ray, D. A., Feschotte, C., Pagan, H. J. T., Smith, J. D., Pritham, E. J., Arensburger, P., Atkinson, P. W., & Craig, N. L. (2008). Multiple waves of recent DNA transposon activity in the bat, *Myotis lucifugus*. *Genome Research*, *18*(5), 717–728. https://doi.org/10.1101/gr.071886.107

Reich, M. S., Shipilina, D., Talla, V., Bahleman, F., Kébé, K., Berger, J. L., Backström, N., Talavera, G., & Bataille, C. P. (2024). Isotope geolocation and population genomics in *Vanessa cardui*: Short- and long-distance migrants are genetically undifferentiated. *bioRxiv*. https://doi.org/10.1101/2023.12.10.569105

Reudink, M., Kyle, C., Nocera, J. J., Oomen, R. A., Green, M. C., & Somers, C. M. (2011). Panmixia on a continental scale in a widely distributed colonial waterbird. *Biological Journal of the Linnean Society*, *102*(3), 583–592. https://doi.org/10.1111/j.1095-8312.2010.01608.x

Richards, G. C. (1990). The spectacled flying-fox, *Pteropus conspicillatus* (Chiroptera: Pteropodidae), in north Queensland. 2. Diet, seed dispersal and feeding ecology. *Australian Mammalogy*, *13*(1), 25–31. https://doi.org/10.1071/am90004

Roberts, B. J., Eby, P., & Westcott, D. A. (2020). *Pteropus conspicillatus.* The IUCN Red List of Threatened Species 2020: E.T18721A22080456. https://dx.doi.org/10.2305/IUCN.UK.2020-3.RLTS.T18721A22080456.en

Roberts, B. J., Catterall, C. P., Eby, P., & Kanowski, J. (2012). Long-distance and frequent movements of the flying-fox *Pteropus poliocephalus*: Implications for management. *PLoS One*, *7*(8), e42532. https://doi.org/10.1371/journal.pone.0042532

Rochette, N. C., Rivera-Colón, A. G., & Catchen, J. M. (2019). Stacks 2: Analytical methods for paired-end sequencing improve RADseq-based population genomics. *Molecular Ecology*, *28*(21), 4737–4754. https://doi.org/10.1111/mec.15253

Roycroft, E., Fabre, P.-H., MacDonald, A. J., Moritz, C., Moussalli, A., & Rowe, K. C. (2022). New Guinea uplift opens ecological opportunity across a continent. *Current Biology*, *32*(19), 4215-4224.e3. https://doi.org/10.1016/j.cub.2022.08.021

Rule, S., Brook, B. W., Haberle, S. G., Turney, C. S. M., Kershaw, A. P., & Johnson, C. N. (2012). The aftermath of megafaunal extinction: Ecosystem transformation in Pleistocene Australia. *Science*, *335*(6075), 1483–1486. https://doi.org/10.1126/science.1214261

Sharbel, T. F., Haubold, B., & Mitchell-Olds, T. (2000). Genetic isolation by distance in *Arabidopsis thaliana*: Biogeography and postglacial colonization of Europe. *Molecular Ecology*, *9*(12), 2109–2118. https://doi.org/10.1046/j.1365-294X.2000.01122.x

Shastry, V., Musiani, M., & Novembre, J. (2025). Jointly representing long-range genetic similarity and spatially heterogeneous isolation-by-distance. *bioRxiv*. https://doi.org/10.1101/2025.02.10.637386

Sheherazade, & Tsang, S. M. (2015). Quantifying the bat bushmeat trade in North Sulawesi, Indonesia, with suggestions for conservation action. *Global Ecology and Conservation*, *3*, 324–330. https://doi.org/10.1016/j.gecco.2015.01.003

Simmons, N. B., & Cirranello, A. L. (2025). Bat Species of the World: A taxonomic and geographic database. Version 1.7. https://batnames.org/

Smyčka, J., Toszogyova, A., & Storch, D. (2023). The relationship between geographic range size and rates of species diversification. *Nature Communications*, *14*(1), 5559. https://doi.org/10.1038/s41467-023-41225-6

Sovic, M. G., Carstens, B. C., & Gibbs, H. L. (2016). Genetic diversity in migratory bats: Results from RADseq data for three tree bat species at an Ohio windfarm. *PeerJ*, *4*, e1647. https://doi.org/10.7717/peerj.1647

Stamatakis, A. (2014). RAxML version 8: A tool for phylogenetic analysis and post-analysis of large phylogenies. *Bioinformatics*, *30*(9), 1312–1313. https://doi.org/10.1093/bioinformatics/btu033

Stange, M., Sánchez-Villagra, M. R., Salzburger, W., & Matschiner, M. (2018). Bayesian divergence-time estimation with genome-wide single-nucleotide polymorphism data of sea catfishes (Ariidae) supports Miocene closure of the Panamanian isthmus. *Systematic Biology*, *67*(4), 681–699. https://doi.org/10.1093/sysbio/syy006

Todesco, M., Pascual, M. A., Owens, G. L., Ostevik, K. L., Moyers, B. T., Hübner, S., Heredia, S. M., Hahn, M. A., Caseys, C., Bock, D. G., & Rieseberg, L. H. (2016). Hybridization and extinction. *Evolutionary Applications*, *9*(7), 892–908. https://doi.org/10.1111/eva.12367

Tsang, S. M. (2015). Phylogeography of Southeast Asian flying foxes (Chiroptera: Pteropodidae: *Pteropus*). PhD thesis, City University of New York. https://academicworks.cuny.edu/gc_etds/1161

Tsang, S. M., Wiantoro, S., Veluz, M. J., Simmons, N. B., & Lohman, D. J. (2018). Low levels of population structure among geographically distant populations of *Pteropus vampyrus* (Chiroptera: Pteropodidae). *Acta Chiropterologica*, *20*(1), 59–71. https://doi.org/10.3161/15081109ACC2018.20.1.004

Tsang, S. M., Wiantoro, S., Veluz, M. J., Sugita, N., Nguyen, Y.-L., Simmons, N. B., & Lohman, D. J. (2020). Dispersal out of Wallacea spurs diversification of *Pteropus* flying foxes, the world's largest bats (Mammalia: Chiroptera). *Journal of Biogeography*, *47*(2), 527–537. https://doi.org/10.1111/jbi.13750

Vanderduys, E. P., Caley, P., McKeown, A., Martin, J. M., Pavey, C., & Westcott, D. (2024). Population trends in the vulnerable grey-headed flying-fox, *Pteropus poliocephalus*; results from a long-term, range-wide study. *PLoS One*, *19*(3), e0298530. https://doi.org/10.1371/journal.pone.0298530

Voris, H. K. (2000). Maps of Pleistocene sea levels in Southeast Asia: Shorelines, river systems and time durations. *Journal of Biogeography*, *27*(5), 1153–1167. https://doi.org/10.1046/j.1365-2699.2000.00489.x

Webb, N. J., & Tidemann, C. R. (1995). Hybridisation between black (*Pteropus alecto*) and grey-headed (*P. poliocephalus*) flying-foxes (Megachiroptera: Pteropodidae). *Australian Mammalogy*, *18*(1), 19–26. https://doi.org/10.1071/am95019

Webb, N. J., & Tidemann, C. R. (1996). Mobility of Australian flying-foxes, *Pteropus* spp. (Megachiroptera): Evidence from genetic variation. *Proceedings: Biological Sciences*, *263*(1369), 497–502. https://doi.org/10.1098/rspb.1996.0075

Welbergen, J. A., Meade, J., Field, H. E., Edson, D., McMichael, L., Shoo, L. P., Praszczalek, J., Smith, C., & Martin, J. M. (2020). Extreme mobility of the world's largest flying mammals creates key challenges for management and conservation. *BMC Biology*, *18*(1), 101. https://doi.org/10.1186/s12915-020-00829-w

Westcott, D. A., McKeown, A., Parry, H., Parsons, J., Jurdak, R., Kusy, B., Sommer, P., Zhao, K., Dobbie, M., Heersink, D., & Caley, P. (2015). Implementation of the national flying-fox monitoring program. Rural Industries Research and Development Corporation, Canberra.

Wiens, B. J., & Colella, J. P. (2024). triangulaR: An R package for identifying AIMs and building triangle plots using SNP data from hybrid zones. *bioRxiv*. https://doi.org/10.1101/2024.03.28.587167

Wiens, B. J., & Colella, J. P. (2025). That's not a hybrid: How to distinguish patterns of admixture and isolation by distance. *Molecular Ecology Resources*, *25*(3), e14039. https://doi.org/10.1111/1755-0998.14039

Wright, S. (1943). Isolation by Distance. *Genetics*, *28*(2), 114–138. https://doi.org/10.1093/genetics/28.2.114

Yi, X., & Latch, E. K. (2022). Nonrandom missing data can bias Principal Component Analysis inference of population genetic structure. *Molecular Ecology Resources*, *22*(2), 602–611. https://doi.org/10.1111/1755-0998.13498

Zhang, G., Cowled, C., Shi, Z., Huang, Z., Bishop-Lilly, K. A., Fang, X., Wynne, J. W., Xiong, Z., Baker, M. L., Zhao, W., Tachedjian, M., Zhu, Y., Zhou, P., Jiang, X., Ng, J., Yang, L., Wu, L., Xiao, J., Feng, Y., … Wang, J. (2013). Comparative analysis of bat genomes provides insight into the evolution of flight and immunity. *Science*, *339*(6118), 456–460. https://doi.org/10.1126/science.1230835

Zheng, X., Levine, D., Shen, J., Gogarten, S. M., Laurie, C., & Weir, B. S. (2012). A high-performance computing toolset for relatedness and principal component analysis of SNP data. *Bioinformatics*, *28*(24), 3326–3328. https://doi.org/10.1093/bioinformatics/bts606